ABSTRACT

Mangroves are recognized as a highly valuable resource due to their provision of multiple ecosystem services. Mapping and monitoring mangrove ecosystems is a crucial objective for tropical region. Thai Binh province is one of the most important mangrove ecosystem in Vietnam. The mangrove ecosystem in this area faces the threat of deforestation from urban development, land reclamation, increase in tourism and natural disasters (global warming). On other hand, a large mangrove area are planted in this area. The aim of this research to detect the changing of mangrove area and mapping the aboveground biomass in Thai Binh province. It also aimed at determining the changes that has occurred over the years 1998, 2003, 2007, 2013 and 2018. The land use land change map was obtained by using supervised classification. The accuracy assessment for the classified images of 1998, 2003 and 2007, 2013 and 2018 are 93%, 86%, 96%, 94% and 91% respectively with kappa of 0.88, 0.79, 0.93, 0.91 and 0.87. The mangrove cover in 1998 was 5874.93ha, in 2003, it increased to 5935.77ha but in 2007, it decreased to 4433.85ha, increased to 6345.09 in 2013 and further increased in 2018 to 6587.88ha. This study also estimate AGB by using vegetation indices. In 1998, the total AGB in this study area are 62880 ton and in 2018 are 187990ha with the root mean square error (RMSE) = 7.2 ton/ha.

TABLE OF CONTENT

LIST OF FIGURE

LIST OF TABLE

LIST OF ABBREVIATIONS

ETM	Enhanced Thematic Mapper
FAO	Food and Agricultural Organization
GIS	Geographic Information System
GPS	Global Positioning System
NDVI	Normalized Difference Vegetation Index
RGB	Red Green Blue
TM	Thematic Mapper
UTM	Universal Transverse Mercator
NIR	Near Infrared
USGS	United States geological survey
MLC	Maximum likelihood classifier
NIR	Near infra-red
RMSE	Root Mean Square Error
AGB	aboveground biomass
GLOVIS	Global Visualization Viewer
AOI	area of interest
SLC	Scan Line Corrector
OLI	Operational Land Imager

CHAPTER 1: INTRODUCTION

1.1 Background

Mangroves are the complex ecosystems that have the unique condition. It has specific characters of flora and fauna, which live in land and salt water habitats in the same time between tidal and low tide boundaries. Mangroves are amongst the most important and productive coastal resources that link terrestrial and marine systems and provide valuable ecosystem goods and service (Alongi, 2002).They typically dominate in the coastal zone of low energy tropical and subtropical coastlines. Mangroves not only importance role in ecosystem but also define an economic resource for the local communities (Kamal & Phinn, 2011). Mangroves can be stabilizing shorelines and having devastating impact of natural such as dissipated the incoming wave energy, trapping sediment in their roots, protecting the land behind, becoming a barrier against wind. They also provide important ecological and social well-being though ecosystem services. They provided essential nursery habitat for fish, crabs, and shrimp (Giri, Pengra, Zhu, Singh, & Tieszen, 2007).

Mangroves forest are the highest biodiversity in all of coastal wetland. Mangroves plant are salt tolerant species, thrive in water that varies in tonnage and is rich with nutrients. According Aubreville (1970) “mangroves” or “mangals” are coastal tropics and found along the sea border, lagoon and river bank where is submerged in brackish water or cover by salt water in high tide (Puri, Gupta, Meher-Homji, & Puri, 1989). Mangroves represented by the concept: mangrove are community of evergreen trees and shrubs of different mangrove species but they have the similar about physiological characteristics and their structure adapt to coastal line habitat and tidal activity, that communities are often growth in tropical and sub-tropical area (Syed, Hussin, & Weir, 2001). Mangrove forests trap sediments flowing down rivers and off the land by virtue of their dense root system and this helps stabilize the coastline and prevents erosion.

Likewise mangroves not only importance role in ecosystem but also define an economic resource for the local communities (Rönnbäck, 1999). For instance, just the fact that many peoples want to live in coastal regions because of economically and aesthetically. The resources of coastal zone provide numerous job opportunities and some peoples come to coastal area for recreation. In the other hand, many pressures could exert on the coastal zone. Some of these are part of natural operation and the effects of human-induced by activities. However, there are limits to extent to which the coastal ecosystem can withstand external assault to its integrity. Pressures emanating from human activities are particularly threatening.

A major driving force of mangrove forests loss in Southeast Asia and in Vietnam is the rapid expansion of aquaculture development. In recent years, mangrove forests have become threatened by development as in Thai Binh, so mangroves have been lost due to coastal development (Alongi, 2002). Therefore, mapping their distribution and areal extent in Vietnam and elsewhere is important for their conservation and management.

Appropriate and cost effective methods are required to reduce the laborious method of manually calculating for the amount of biomass. Remote Sensing (RS) is noted for giving a good classification of mangroves. Therefore, using Remote sensing (RS) and Geographic Information System (GIS) will be an appropriate choice (Sellers et al., 1995). Christensen (1993) was shown that biomass can be evaluate by Deriving light interception from spectral reflectance ratio (Christensen & Goudriaan, 1993). The biomass in a large area can be compute by using remotely sensed satellite data to save time and money (Tripathi, Soni, Maurya, & Soni, 2010). This research is based on the integration of RS and GIS in estimating the spatial extent of mangrove and the rate of change of mangrove in the costal line of Thai Binh province. It also estimate how much above ground biomass in mangroves in the study area.

1.2 Prior study

Several research work have been carried out in this field of research. Dat (2011) Monitoring mangrove forest using multi-temporal satellite data in the Northern Coast of Vietnam (Dat & Yoshino, 2011), Pham Tien Dat (2012) were to analyse the current status of mangroves using different ALOS sensors in Hai Phong, Vietnam in 2010 and compare the accuracy of the post satellite image processing of ALOS imagery in mapping mangroves (Pham & Yoshino, 2012). The research about implementation of mangrove management investigated by the authorities, community or local people has affected mangrove change in Vietnam (Pham & Yoshino, 2016).

Beland (2006) describes the use of a proposed change detection methodology in the assessment of mangrove forest alterations caused by aquaculture development, as well as the effectiveness of the measures taken to mitigate deforestation in the district of Giao Thuy, Thai Binh Vietnam, between 1986, 1992 and 2001 (Beland, Goita, Bonn, & Pham, 2006). Mazda (1997) give the demonstrate the usefulness of mangrove reforestation for coastal protection in Thai Binh province (Mazda, Magi, Kogo, & Hong, 1997). Nguyen Hai Hoa (2016) was using Landsat imagery and vegetation indices differencing to detect mangrove change (Hoa).

1.3 Role of remote sensing and GIS in mangrove monitoring

Earth observing by using satellite remote sensing has made it possible to collect data globally in a relatively short time and for these observations to be continued in the future. Remote sensing system can record the biological and physical data; therefore we can use that data for forest inventory and environment monitoring. It could be support by Global Position System (GPS) in collecting ground data and truth data in the earth surface (Parkinson, 2003).

A first step towards dealing with important environmental issues is to produce relevant and up-to-date spatial information that may provide a better understanding of the problems and form the basis for the identification of suitable strategies for sustainable development. In this point, Remote Sensing and GIS are potentially can process the mapping in order to monitor the mangroves (Green, Clark, Mumby, Edwards, & Ellis, 1998).

Remote sensing is an important substitute for traditional field monitoring for managing large-scale mangroves (Blasco et al., 1998). Aerial photographs and high-resolution satellite images are the main sources of remote sensing data for mangrove mapping. Satellite data with medium or low resolution and laser scanning data are other remote sensing data sources that can be used to assess mangrove ecosystems. In the scientific literature, there are a considerable number of studies related to mangrove forests, remote sensing data and various image-processing algorithms.

Most of the remote sensing studies use high-resolution spatial images, mainly with pixel sizes of 5 to 100 m. Image processing and imaging algorithms have a significant impact on the accuracy of mangrove forest maps. Therefore, it is imperative to identify appropriate sources of data and precise methods for processing mangrove forests. When applying pixel based classification algorithms, there are some limitations. Misalignment of mangrove forests, non-mangrove vegetation, urban areas and even mudflats affect classification accuracy (Gao, 1998).

According Green (1998) Remote-sensing techniques have demonstrated a high potential to detect, identify, map, and monitor mangrove conditions and changes. Also, climate change-related remote-sensing studies in coastal zones have increased drastically in recent years (Green et al., 1998). Remote sensing techniques offer timely, up-to-date, and relatively accurate information for sustainable and effective management of wetland vegetation. They also applications in discriminating and mapping wetland vegetation, and estimating some of the biochemical and biophysical parameters of wetland vegetation (Adam, Mutanga, & Rugege, 2010).

1.4 Problem Statement

Meanwhile, various ongoing activities will greatly affect to coastal area and mangrove and then long-term cumulative impacts will become more evident. Coastal areas are inter-land and seashore interchanges that are unique geologic, ecological, and biological sites of vital importance for a wide range of terrestrial and marine life forms including human (Beatley, Brower, & Schwab, 2002). Coastal ecosystems are very fragile due to the variability of tectonic and terrain processes and variability.

Vietnam's coastal regions are constantly experiencing changes by the impact of nature as well as human activities. Mangroves is a sensitive ecosystem, which vulnerable by environmental change include sea level rise and hydrological changes in coastal areas (Mitra, 2013).Nevertheless, mangroves are under severe threat. High population growth, and migration into coastal areas, hasled to an increased demand for its services. The situation is further exacerbated by weak governance, poor planningand uncoordinated economic development in the coastal zone. Globally more than 3.6 million hectares of Mangroveshas been lost since 1980. In Vietnam, it is estimated that the number of mangrove forest was about 400,000 hectares in early 20th century. However, this number declined dramatically over 50 years (T. Q. Vo, Kuenzer, & Oppelt, 2015).

Since Remote Sensing (RS) technology provides data from which updated land cover information cheaply and also it can be extracted efficiently. Thus, land use change detection has become a major application of remote sensing data and can apply to identify the changing in mangrove in Vietnam (Muchoney & Haack, 1994).

Maintaining mangrove ecosystem services and a healthy environment is one of the priority goals of the Vietnam government. Although many studies about mangrove forest have been done in Thai Binh province to understand the valuable of this ecosystems, but some knowledge gaps still exist. In particular, baseline mangrove data need to be updated, in addition to providing an indication of the species that are vulnerable, death, or changes to drainage due to urban and rural developments.

Therefore, it is necessary to monitor mangrove forest, and mapping of mangroves is important in order to support coastal zone management and planning programs.

1.5 Research Objectives

The goals of this research is mapping out mangrove forest from 1998 to 2018. It further aims at determining the amount of above-ground biomass in mangrove using allometric equations and Remote Sensing.

The primary objective can be subdivided into following tasks:

- Mapping mangrove forest and using RS and GIS and assess of mangrove forest change using Remote Sensing
- Estimate amount of aboveground biomass by different vegetation index within study area.
- Assessing the accuracy of each AGB estimation model.

- Estimate the changing of aboveground biomass from 1998 to 2018 within study area.

1.6 Organization of the Thesis

The content of the research is structured under the following chapters:

Chapter I: Chapter 1 introduces the research work. It highlights on prior research work based on mangrove above ground biomass. The objectives of the research is highlighted within this chapter. This chapter also show the problem statement and research question.

Chapter II: Chapter 2 gives a theoretical and conceptual of mangrove. Literature review on mangroves and further talks about climate change, effect of climate change to mangrove. This chapter further researches on the various RS methods that have been employed in similar study.

Chapter III: Chapter 3 gives the method about establish survey pots, collecting data, analysis data, estimate above ground biomass and change detection.

Chapter IV: Chapter 4 shows the results obtained from the research. Analysis and discussions are carried out on the result.

The conclusions and recommendations drawn from the research are presented in chapter five.

CHAPTER 2: LITERATURE REVIEW

2.1 Mangroves

Mangrove forest have been described by many authors over time and the literature (for example (M. Spalding, Kainuma, & Collins, 2010), (FAO, 2007)). Mangrove forests literally live in two worlds at once. Mangroves are comprised of salt-tolerant tree or shrub species growing in the intertidal areas and estuary mouths between land and sea. They thrive in intertidal region (includes: sheltered coastlines, shallow-water lagoons, estuaries, rivers or deltas) (MAP, 2013). Mangroves are found in the tropical and subtropical regions of the world between approximately 30°N and 30°S latitude (FAO, 2007). The total species of mangroves forest are 54-75 species, which are found only in the intertidal zone of coasts. There species are highly adapted to intertidal environment, capable of expelling salt, allowing mangroves to thrive in saline waters and soils. Mangroves are found worldwide, but the greatest species diversity is in Southeast Asia (MAP, 2013).

The total area of mangroves in the year 2000 was 137,760 km^2 in 118 countries and territories in the tropical and subtropical regions of the world. The largest extent of mangroves is found in Asia (42%) followed by Africa (20%), North and Central America (15%), Oceania (12%) and South America (11%). Approximately 75%of mangroves are concentrated in just 15 countries (Giri et al., 2011)

In recent years, the area and the quality of mangrove forest was decreased in Thai Binh province, especially in in the period 1995 – 2000 because the changing land use from mangrove forest to aquaculture farm. The land and forest area in coastal line of Thai Binh province are 9,167 ha therein forest area is 3,709 ha and non-forest area is 5,908 ha. In the low tide area, the percent of sand in soil from 83.64% to 86.57% some area can reached 98.32%. In the high tired area, the rate of sand in soil from 39.19% to 43.69% (Đỗ Quý & Bùi Thế, 2018).

2.2 Physical factors affecting the growth of Mangroves

There are some important biological and abiotic factor influence to develop of mangroves. That factor formed specific characteristic of mangroves forest. They include:

2.2.1 Climatic factor

Mangrove ecosystems are threatened by climate change. The state of knowledge of mangrove vulnerability and responses to predicted climate change and consider adaptation options. All the climate change outcomes, relative sea-level rise may be the greatest threat to mangroves. Most mangrove sediment surface elevations are not keeping pace with sea-level rise, although longer-term studies from a larger number of regions are needed. Rising sea-level will have the greatest impact on mangroves experiencing net lowering in sediment elevation, where there is limited area for landward migration (Gilman, Ellison, Duke, & Field, 2008).

2.2.2 Temperature

The mean annual temperature in the South coastal is about 27^0C and decreases northwards to about 21^0C in the North coastal. Cold air was brought by the northeast monsoon to the north, there by affecting the growth and composition of mangroves in this region (Lugo & Patterson-Zucca, 1977).Mangrove species are largest size and the most abundant in the equatorial and subtropical areas, where annual temperatures are high and narrow temperature range. The appropriate temperature and about 25^0C-30^0C as in the southern provinces of Vietnam. The number of mangrove species and mangrove forest tree in the north is generally lower or smaller than in the south of Vietnam, partly because of the low temperature in winter and the high temperatures in summer. High temperatures or sudden fluctuations in temperature, can also have an adverse effect on mangrove.

2.2.3 Precipitation

The distribution and growth of tropical forest are mostly in equatorial areas where the rainfall is high (about 1800-2500mm/year). Precipitation is the main factor for the distribution of mangroves forest in different tired areas (Eslami-Andargoli, Dale, Sipe, & Chaseling, 2009). Mangroves require a certain amount of fresh water for optimum growth, even though they are salt tolerant species. Rain regulates salt concentration in soil and plants and provides an extra source of fresh water, in addition to river water, for mangroves and this favours their physiological processes. In

Vietnam, there are about 100 rainy days per year with average rainfall of 1.500 to 2.000 mm and air humidity of less than 80%.

Southwest monsoons from the ocean bring heavy rain to Vietnam during the summer months. Consequently, the most dense mangrove forest are found in this region. For instance, mangroves flourish at Ca Mau cape, where rainfall are 2000-2200 mm annually with 120-150 rainy days per year. On the other hand, mangroves are sparse along the small estuaries of Khanh Hoa coast where they receive less than 1000 mm/years ("AccuWeather," 2018)

2.2.4 Waves and tidal range

Even though mangrove can survey and develop with waves and tide activity but mangrove propagules and seedlings require a low energy habitat. Therefore, mangroves often grow in sheltered shores areas. Surface slope and tidal range will determine the area and distribution of mangrove, with large tide range and large tide area mangrove will be larger (De Vos, 2004).

2.2.5 Salinity conditions

Survival declined with decrease in irradiance, except where very low salinities apparently induced sensitivity to high irradiance in vulnerable species. Survival in understorey shade was lower in the high than low salinity environment. However, these apparent effects of salinity were eliminated by reducing below-ground interactions with adult trees (Ball, 2002). For example, *Excoecaria agallocha*species was distribute in low salinity condition area (smaller than 5psu), if salinity from 5-15 will be reduce the rooting growth of seed, when the salinity higher than 15psu the seed will not rooted. Salinity also effect to the ability of leaves growing and leave area, high salinity will make lower in mangrove height and leave area will be smaller. High salinity also decrease the longevity of leave and reduce the ability of leave born, it lead to mangrove will dead in long term (Chen & Ye, 2014).

2.2.6 Soil structure

Soil condition is also effect to the distribution of dominate mangrove species (McKee, 1993). The condition for develop mangrove in the area with substrate, waterlogged, anaerobic as sediments, sand and coarse sand, peat soil or coral reef. However, the best condition for mangrove forest are living in silty clay soils (Hong & San, 1993). Mangroves soil is formed by alluvial, sediment from rivers and sea with rich of nutrients such as magnesium, sodium. The soil physical and chemical characteristic depend on the sources of alluvial and sediments, therefore it effect to the distribution of mangrove forest (Tam & Wong, 1996).

2.3 The Application of Remote Sensing in monitoring Mangroves

In recent year, many researches have shown that remote sensing are important tool for mangrove forest research with low cost in a large scale (Giri et al., 2011; Giri et al., 2007; Winarso et al., 2017). Remote sensing data often use for change detection and monitor mangroves forest. Remote sensing is science that collect information about object, area or a phenomenon in the world though analysis the data obtained by using device that is not exposed to the object, area or phenomenon under investigation as satellite or radar. Remote sensing has been identified as a cost-effective method using in a large area and even a geographic areas. They have a great effect in monitoring the change of vegetation especially in forest sector research (Lillesand, Kiefer, & Chipman, 2014).

Data on vegetation cover change is important with planners for monitoring effect of vegetation change in local level or in the world. That data are valuable for resource management and planning for evaluate the changing of vegetation and anticipate changes in the future. According to Macleod et al (1998) four important aspects of change detection in natural resource monitoring: detecting the change have occurred, determining the essence of change, measuring the change and assessing the spatial pattern of change (Macleod & Congalton, 1998).

The applications of RS and GIS provide various guidelines for the sustainability of management of tropical coastal ecosystems, including mangroves. It shows that remote sensing technology can be integrated in long-term studies combining the past and present to make predictions about the future and, if necessary they can show the action to prevent degradation of natural resources. Especially, they have been used to study mangroves (Ramachandra & Ganapathy, 2007). For the large mangroves forest study, high-resolution satellite image can be show the forest structure characteristic. These results can be used to predict future changes in forest structure. (Dahdouh-Guebas, 2001).

The essence of using remote sensing data to detect mangrove forest cover changing is detection change in radiance value, which can recognize through remotely sensed. Nowadays, the technique of using remote sensing images to detect change has grown very rapidly following the development of computers. Coppin et al (1996) summarized 10 types of techniques used to detect the change they include: Mono-temporal change delineation, delta or post classification comparisons, multi-dimensional temporal feature space analysis, and composite analysis. Others are image differencing, multi-temporal linear data transformation, change vector analysis, image regression, multi-temporal biomass index NDVI, background subtraction, and image rationing (Coppin & Bauer, 1996)

2.3.1 Aerial photography

Aerial photography (AP) and high-resolution image system as Landsat and sentinel are the most common approaches to mangrove remote sensing (Newton et al., 2009). AP has been widely used in mangrove mapping and assessment. AP can be more cost effective over small areas than satellite remote sensing. Anderson (1997) found aerial photographs still useful in mapping wetlands. Furthermore, aerial photographs are relatively cheap to analyse especially if the areas covered are small, such as mangroves and the AP can provide a quick assessment to detect the change (M. D. Spalding, Blasco, & Field, 1997)

In aerial mapping, many limitations that can affect the outcome of the product. The major limitation are the limited areal extent and relatively high costs of data for large geographic areas. Some limitation related to the sensor, the airborne platform, the environment, the interpreter user of the information (Witenstein, 1955).

2.3.2 Satellite imagery

The vast majority of mangrove remote sensing studies have employed high-resolution satellite imagery such as Landsat (MSS, TM, or ETM+), SPOT (HVR, HRVIR, or HRG), ASTER, or IRS (1C or 1D).The techniques used to detect and classify mangroves forest are unsupervised classification techniques such as the ISODATA approach, supervised classification techniques such as the maximum likelihood classification (MLC), mahalanobis distance, or other techniques commonly available in commercial image processing software, or a hybrid unsupervised/supervised classification scheme (Wilkinson, 2005). The new techniques can improve accuracy of mangrove classification, detect individual species, and provide reliable estimates of structure such as leaf area, canopy height, and biomass (Heumann, 2011)

2.3.3 GIS, Remote Sensing and Change Detection

The advantage of creation of thematic map using Remote Sensing and Geographical Information Systems (GIS) is effective and efficiency. Both Remote Sensing and GIS techniques are important fields of study particularly in the three major application that are in area of urban growth studies, area of land use change detection analysis, and vegetation studies (NDVI). In this study GIS application, plays significant role in change detection of mangrove forest studies that involves the use of GIS software of both remote sensing and GIS techniques with powerful tools that has the capacities of incorporating different data set particularly in this study.

Definition of Remote sensing refers to Lillesand dan Kiefer (2014) that is the science and art of obtaining information (acquisition) about objects, regions or phenomena by analysing the data obtained by without direct contact with the object, area or phenomenon which being studied (Lillesand et al., 2014). As an information that can analyse, remote sensing can provide a variable source of data updated and land cover information.

2.3.4 Mangrove biomass estimation by Remote Sensing and GIS

While biomass derived from field data measurements is the most accurate, it is not a practical approach for broad-scale assessments. This is where Remote Sensing has a key advantage. It can provide data over large areas at a fraction of the cost associated with extensive sampling and enables access to inaccessible places. Data from Remote Sensing satellites are available at various scales, from local to global, and from a number of different platforms (Kumar, Sinha, Taylor, & Alqurashi, 2015).

Estimates of forest biomass can provide valuable insights into the carbon storage and cycling in forests (Litton, Raich, & Ryan, 2007). Traditional remote sensing approaches can provide important information for monitoring change of mangroves in area. Recent advances in satellite sensors and techniques can potentially improve the accuracy of mangrove classifications, provide reliable estimates of structure such as leaf area, canopy height, detect individual species, and biomass (Heumann, 2011). Remote sensing-based methods of aboveground biomass (AGB) estimation in forest ecosystems have gained increased attention, and substantial research has been conducted in the past three decades (Lu et al., 2016). Proisy, (2007) using Fourier-based textural ordination to estimate mangrove forest biomass from very high-resolution (VHR) IKONOS images. The FOTO method computes texture indices of canopy grain by performing a standardized principal component analysis (PCA) on the Fourier spectra obtained. In addition, a multiple linear regression based on the three main textural indices yielded accurate predictions of mangrove total aboveground biomass (Proisy, Couteron, & Fromard, 2007).

According to Simard, (2006) the application of the elevation data from the Shuttle Radar Topography Mission (SRTM), which was calibrated using airborne LIDAR data and a high resolution USGS digital elevation model (DEM) for produced a landscape scale map of mean tree height in mangrove forests. And then, he using field data to derive a relationship between mean forest stand height and biomass in order to map the spatial distribution of standing biomass of mangroves by applied linear regression (Simard et al., 2006).

Fatoyinbo, (2008) was determine the mean tree height spatial distribution and biomass of mangrove forests using Landsat ETM+ and Shuttle Radar Topography Mission (SRTM) data. The SRTM data were calibrated using the Landsat derived land-cover map and height calibration equations. Stand-specific canopy height-biomass allometric equations developed from field measurements and published height-biomass equations were used to calculate aboveground biomass of the mangrove forests on a landscape scale. (Fatoyinbo, Simard, Washington-Allen, & Shugart, 2008)

Lu, (2016) was provides a survey of current biomass estimation methods using remote sensing data and discusses four critical issues – collection of field-based biomass reference data, extraction and selection of suitable variables from remote sensing data, identification of proper algorithms to develop biomass estimation models, and uncertainty analysis to refine the estimation procedure. Additionally, he also discuss the impacts of scales on biomass estimation performance and describe a general biomass estimation procedure. Although optical sensor and radar data have been primary sources for AGB estimation, data saturation is an important factor resulting in estimation uncertainty (Lu et al., 2016)

CHAPTER 3: METHOD

3.1 Study area

The study area includes the province of Thai Binh, located in northeastern coastal Viet Nam.

3.1.1 Geography location

Thai Binh is an eastern coastal province in the Red River Delta region; the distance with Ha Noi capital is 110 km, with Hai Phong city 70 km and with Nam Dinh city 18 km. This province is a coastal province in the Red River Delta region. The North part border the provinces of Hai Duong, Hung Yen and Hai Phong city ; The South part border Nam Dinh province ; The Western part border Ha Nam province and the Eastern part border Gulf of Tonkin. They being a delta province with flat terrain and slope of below 1 percent; the terrain of Thai Binh province runs downward from the North to the South and varies its height of 1 to 2m to the sea level. In administrative border, over natural land area of province, nowadays there is above 16 thousands ha of Thai Thuy and Tien Hai district's coastal land was measured, today is being invested exploited to aquaculture and afforest, in there, it inserted aquaculture over 4.000 ha and planted 7.000 ha salt-marsh forest.

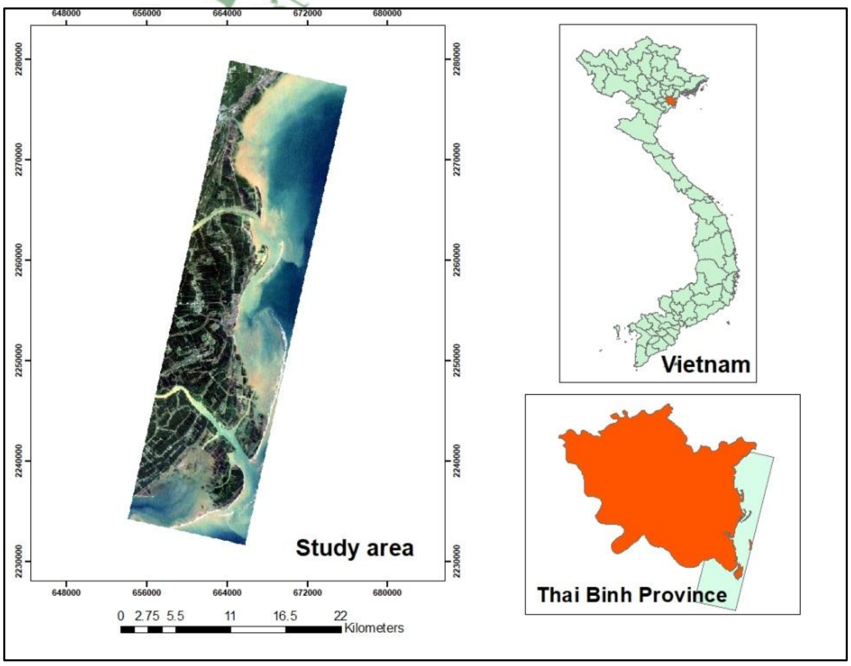

Figure 1: Study area

3.1.2 Climate

This study focused on the Thai Binh province, Vietnam. The province is lie in tropical monsoon area, big heat radiation, create high temperature. Average temperature from 23^oC to 24^oC this temperature are good for the development of mangrove. Thermal amplitude in season is 13^oC with the temperature of 3 month are lower than 20^oC, in January and February the lowest temperature can be lower than 5^oC. This factor will be effect to the development of mangrove (Cúc, 2013).

Average rainfall in year from 1.500 millimetre to 1.900 mm in a year maximum rainfall in August and September, this precipitation is lower than the suitable rainfall for mangrove (Yinxia, 1995). In winter the precipitation are lower than 30 mm/month; average moisture is 85% - 90%.

3.1.3 Tidal regime

The plain is affected by diurnal tide of Tonkin gulf with tidal range of approximately 4m. In a day, there is one high tide and one low tide and in one month, one spring tide and one neap tide occur. The tidal range tends to decrease slightly from north to south as well sea to rivers inland but not so much due to short distance between two ends of estuaries. The highest water level recorded at Hon Dau (Hai Phong) was 2,66m above MSL (October, 1955) and lowest level was - 1.62m (January, 1969). (Cat & Duong, 2006).

3.1.4 Mangroves forest in Thai Binh Province

3.1.4.1 Status mangroves in Thai Binh Province

The area of mangrove forest in Thai Binh province are low compare with total area of province but they have important roles in food chain, protecting coastal area, economic value for local people. Most of mangrove forest in study site are plantation mangrove. The percent of natural mangrove area low and they dispersed distribution. Almost mangrove are planted by funding from international organizations, just a small area planted by funding of Vietnam government. (Cúc, 2013)

Thai Binh mangrove forest distributed in the coastal area of 10 communities belong to Thai Thuy and Tien Hai district. The mangrove area in Thai Thuy district is 2000ha and in Tien Hai district are 1400 ha. (Thuy et al., 2016)

Thai Binh coastal area have 12 species include: *Acrostichum aureum,Acathus ebracteatus,Acathus ilicifolus , Sensuvium portulacastrum, Avicennia marina, Lumnitzera racemose, Derris trifoliata, Excoecaria agallaocha, Aegiceras corniculatum, Bruguiera gymnorrohiz, Kandelia obovate, Rhizophora stylosa, Sonneratia caseolaris (Cúc, 2013).*

3.1.4.2 Effect of climate to mangroves in mangroves forest

There are some climate factor that effect to the development of mangrove forest are:

Firstly, the effect of low temperature because of cold winter: The winter season from December to February of next year. The lowest temperature often occur in January with temperature lower than 15^0C and absolute minimum temperature < 5^0C. Mangrove have low increasing rate in this season, some mangrove was dead because of low temperature.

Secondly, the effect of storms and tropical depressions: Mangrove in Thai Binh are often effect by the activities of storms and tropical depressions. When the storm landed in the mainland, wind speed can reach 40-50 m/s, waves 5-7 m high, especially when tides, often cause very serious consequences: broke mangrove tree, change the salinity, seedling are submerged,…

3.2 Data collection

In this study, we collected two type of data field survey data and satellite image data to detect mangrove change and estimate above ground biomass.

3.2.1 Instruments and software

The following list of instruments used for the fieldwork and the software used for this study (see Table 1)

Table 1: Instrument and Software are used

No.	Type	Name	Utility
1	Instrument	GPS: Garmin 7 channel	Collecting ground truth coordinates
2	Instrument	Diameter Tape	Diameter Measurement
3	Instrument	Measuring tape 50 meter	Length of measurement
4		Field Datasheet	Recording field data
5	Software	Arc GIS 10.2	Image processing and data analysis, Spatial analysis Principal Component Analysis
6	Software	MS Word	For documental
7	Software	MS Excel	Data analysis
8	Software	Envi 5.3	Image pre-processing and data analysis, classification data.
9	Software	SPSS 23	Data analysis

3.2.2 Satellite image collection

In this study, satellite image were obtained from the United States Geological survey (USGS) Global Visualization Viewer (GLOVIS) free of charge include Landsat image and sentinel image. Image obtained are dated 1998, 2003, 2007, 2013 and 2018 as described in Table 2. Landsat image was obtained from Landsat constellation of satellites that each had a resolution of 30 meters. The area of interest (AOI) for this study is located within the dataset of WRS (World Reference System) path 126 and Row 46 with correction level 1-T. The sensors on board the Landsat Satellites records the surface reflectance of electromagnetic (EM) radiation from the sun in seven discreet bands (Table 3 and Table 4).

Sentinel 2 image was obtained from a constellation of two satellites, both orbiting Earth at an altitude of 786 km and they had a resolution of 10 meters. The research was based on a decadal analysis of images but due to lack of clear images of cloud cover less than 10%. SENTINEL-2 data are acquired on 13 spectral bands in the VNIR and SWIR. The satellite image in this study was used in this research describe below:

Table 2: Satellite Images Used in Research

No	Date of image acquisition	Satellite	Resolution	Path/row
1	02/11/1998	LT05_L1TP_126046_19980929_20161221_01_T	30x30	126/46

		1		
2	21/10/2003	LE07_L1TP_126046_20031021_20170123_01_T1	30x30	126/46
3	02/02/2007	LE07_L1TP_126046_20070202_20170105_01_T1	30x30	126/46
4	08/10/2013	LC08_L1TP_126046_20131008_20170429_01_T1	30x30	126/46
5	07/05/2018	S2A_MSIL1C_20180705T031541_N0206_R118_T48QXH_20180705T061521	10x10	

Sources: https://earthexplorer.usgs.gov/

3.2.2.1 Landsat 5 Thematic Mapper (TM) and Landsat 7 Enhanced Thematic Mapper Plus (ETM+)

The Landsat Thematic Mapper (TM) sensor was carried onboard Landsat 5 from July 1982 to May 2012 with a 16-day repeat cycle, referenced to the Worldwide Reference System-2. Very few images were acquired from November 2011 to May 2012. The satellite began decommissioning activities in January 2013.

Landsat 5 TM image data files consist of seven spectral bands (See Table 3). The resolution is 30 meters for bands 1 to 7. (Thermal infrared band 6 was collected at 120 meters, but was resampled to 30 meters.) The approximate scene size is 170 km north-south by 183 km east-west (106 mi by 114 mi). (Chander, Markham, & Barsi, 2007)

Most Landsat 5 TM scenes are processed through the Level 1 Product Generation System (LPGS), processed to full Precision Terrain correction. Some TM scenes do not have the ground-control or elevation data necessary to perform these corrections.

Landsat 5 Thematic Mapper (TM) scenes held in the USGS archive can be searched using EarthExplorer, the USGS Global Visualization Viewer (GloVis), or the LandsatLook Viewer. On EarthExplorer, Landsat 4-5 TM scenes can be found under the Landsat menu in the “Landsat Collection 1 Level-1” section, in the “Landsat 4-5 TM C1 Level-1” dataset.

The Landsat Enhanced Thematic Mapper Plus (ETM+) sensor onboard the Landsat 7 satellite has acquired images of the Earth nearly continuously since July

1999, with a 16-day repeat cycle. All Landsat 7 scenes collected since May 30, 2003 have data gaps due to the Scan Line Corrector (SLC) failure. Landsat 7 scenes acquired after this date are categorized as SLC-off. Landsat 7 ETM+ images consist of eight spectral bands with a spatial resolution of 30 meters for bands 1 to 7. The panchromatic band 8 has a resolution of 15 meters. All bands can collect one of two gain settings (high or low) for increased radiometric sensitivity and dynamic range, while Band 6 collects both high and low gain for all scenes. Approximate scene size is 170 km north-south by 183 km east-west (106 mi by 114 mi). The ETM+ produces approximately 3.8 gigabits of data for each scene. An ETM+ scene has an Instantaneous Field Of View (IFOV) of 30 meters x 30 meters in bands 1-5 and 7 while band 6 has an IFOV of 60 meters x 60 meters on the ground and the band 8 an IFOV of 15 meters. Please visit the L7 Science Data Users Handbook for a detailed description of ETM+ spatial characteristics. (Heckenlaible, Meyerink, Torbert, & Lacasse, 2007).

Table 3: The Band Designations for Landsat 5 Thematic Mapper (TM) and Landsat 7 Enhanced Thematic Mapper Plus (ETM+)

	Bands	Wavelength (micrometers)	Resolution (meters)
Landsat 7 Enhanced Thematic Mapper Plus (ETM+)	Band 1 - Blue	0.45-0.52	30
	Band 2 - Green	0.52-0.60	30
	Band 3 - Red	0.63-0.69	30
	Band 4 - Near Infrared (NIR)	0.77-0.90	30
	Band 5 - Shortwave Infrared (SWIR) 1	1.55-1.75	30
	Band 6 - Thermal	10.40-12.50	60 * (30)
	Band 7 - Shortwave Infrared (SWIR) 2	2.09-2.35	30
	Band 8 - Panchromatic	.52-.90	15

Source: (Barsi, Lee, Kvaran, Markham, & Pedelty, 2014)

3.2.2.2 Landsat 8

The Operational Land Imager (OLI) and Thermal Infrared Sensor (TIRS) are instruments on board the Landsat 8 satellite, which was launched in February of 2013. The satellite collects images of the Earth with a 16-day repeat cycle, referenced to the Worldwide Reference System-2. The spectral bands of the OLI sensor, while similar to Landsat 7's ETM+ sensor, provide enhancement from prior Landsat instruments, with the addition of two new spectral bands: a deep blue visible channel (band 1) specifically designed for water resources and coastal zone investigation, and a new infrared channel (band 9) for the detection of cirrus clouds. Two thermal bands (TIRS) capture data with a minimum of 100 meter resolution, but are registered to and delivered with the 30-meter OLI data product. (See Table 4) Landsat 8 file sizes are larger than Landsat 7 data, due to additional bands and improved 16-bit data product (Mission).

Table 4: The Band Designations for the Landsat 8 Satellites

Landsat 8	Bands	Wavelength (micrometer)	Resolution (meters)
Operational Land Imager (OLI) and Thermal Infrared Sensor (TIRS)	Band 1 - Ultra Blue (coastal/aerosol)	0.435 - 0.451	30
	Band 2 - Blue	0.452 - 0.512	30
	Band 3 - Green	0.533 - 0.590	30
	Band 4 - Red	0.636 - 0.673	30
	Band 5 - Near Infrared (NIR)	0.851 - 0.879	30
	Band 6 - Shortwave Infrared (SWIR) 1	1.566 - 1.651	30
	Band 7 - Shortwave Infrared (SWIR) 2	2.107 - 2.294	30
	Band 8 - Panchromatic	0.503 - 0.676	15
	Band 9 - Cirrus	1.363 - 1.384	30
	Band 10 - Thermal Infrared (TIRS) 1	10.60 - 11.19	100 * (30)
	Band 11 - Thermal Infrared (TIRS) 2	11.50 - 12.51	100 * (30)

Source: (Barsi et al., 2014)

3.2.2.3 Sentinel 2:

SENTINEL-2, launched as part of the European Commission's Copernicus program on June 23, 2015, was designed specifically to deliver a wealth of data and imagery. The satellite is equipped with an opto-electronic multispectral sensor for surveying with a sentinel-2 resolution of 10 to 60 m in the visible, near infrared (VNIR), and short-wave infrared (SWIR) spectral zones, including 13 spectral channels (see Table 5), which ensures the capture of differences in vegetation state, including temporal changes, and also minimizes impact on the quality of atmospheric photography. The orbit is an average height of 785 km and the presence of two satellites in the mission allow repeated surveys every 5 days at the equator and every 2-3 days at middle latitudes (Sentinel).

Table 5: Wavelength Regions and Description of Each Sentinel Band

Band name	Resolution (m)	Central wavelength (nm)	Band width (nm)	Purpose
B01	60	443	20	Aerosol detection
B02	10	490	65	Blue
B03	10	560	35	Green
B04	10	665	30	Red
B05	20	705	15	Vegetation classification
B06	20	740	15	Vegetation classification
B07	20	783	20	Vegetation classification
B08	10	842	115	Near infrared
B08A	20	865	20	Vegetation classification
B09	60	945	20	Water vapour
B10	60	1375	30	Cirrus
B11	20	1610	90	Snow/ ice / cloud discrimination
B12	20	2190	180	Snow / ice / cloud discrimination

Source: (sentinel.esa.int, 2018)

3.2.3 Field survey

Fieldwork is a very important part of the research. Fieldwork helps to check and collect most of the ground information require for mapping. The purpose of sampling is to obtain ground truth data and measure the AGB of the study area. Ground truth data were collected using a Garmin handheld GPS for training data and accuracy assessment, Google earth image can be used for visual inspection. Tree measurement data also collected in fieldwork. The data was collected base on random selection method with in area of study (Cornelius, Sear, Carver, & Heywood, 1994).

3.2.3.1 Ground truth data survey.

Ground truth data is a term used to refer to information collected "on location" to verify a satellite image pixel within a certain area. To be more specific it refers to a process in which pixels from Landsat or other satellite images are compared to the actual or real object on the ground that can be used to verify the pixel of an image. In the case of classified images it will help to determine the accuracy of the image performed by remote sensing software.

Transect lines were made along the study area. GPS: Garmin 7 channel was used for record position of habitat type position in transect. Due to the marshy grounds, accessibility to some part of the mangrove forest was not possible hence a uniformed distance for choosing sites along the transect line was not achieved.

3.2.3.2 Sample Size and Sampling Techniques

Sampling plots can be of any size and shape. It can be either square, circle or rectangle. However, circular plots are commonly used in forest inventory (Wenger, 1984).Circular plots are easier to establish than other plots because only one point, the centre of the plot is defined and the radius of the plot is measured from the centre and the parameter is determined. In this study, circular plot of 1000m^2 with radius 17.8m from the centre of the plot was established (Figure 2).

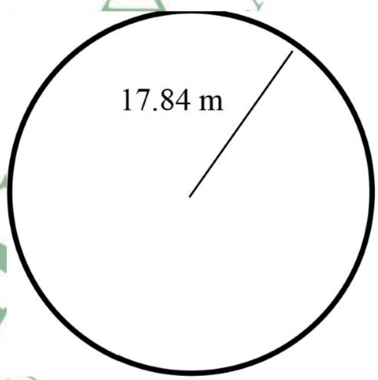

Figure 2: Circular plot of 1000 m²

3.2.3.3 Field data collection

Height and DBH or Diameter at 0.3m height ($D_{0.3}$) measurements have been the key parameters for estimating aboveground biomass and carbon (Brown, 1997). Identification of all species within the sampling was made. In addition, diameter at breast height (DBH) and total height (H) of all individual species with ≥ 5 cm DBH were measured. Tree diameter was measured at 1.3 m aboveground or 30 cm above the tallest buttress/prop roots if taller than 1.3 m. In case a tree forks below 1.3 m from the ground, all stems with ≥ 5 cm DBH were measured separately (Tobias et al., 2017). For *Kandelia cande* species Diameter at 0.1 was measured in every tree (Khan, Suwa, & Hagihara, 2005) The procedure of data collection is crucial in the field.

Consequently, measurement of DBH, $D_{0.3}$ height and species identification of all trees crown cover percentage and sample centre coordinates were recorded in every sample plots. The coordinates of the centre of the plots were recorded using the GPS.

Field data were collected in March 2018 in the coastal line of Thai Binh province. The location of the sample plots was restricted to easily accessible areas based on simple random sampling. Tree parameters such as diameter at breast height (DBH) and height were recorded individually. All trees with DBH or $D_{0.3} \geq 1$ cm in the sample plot were measured using diameter tape at 30 cm above the highest prop roots.

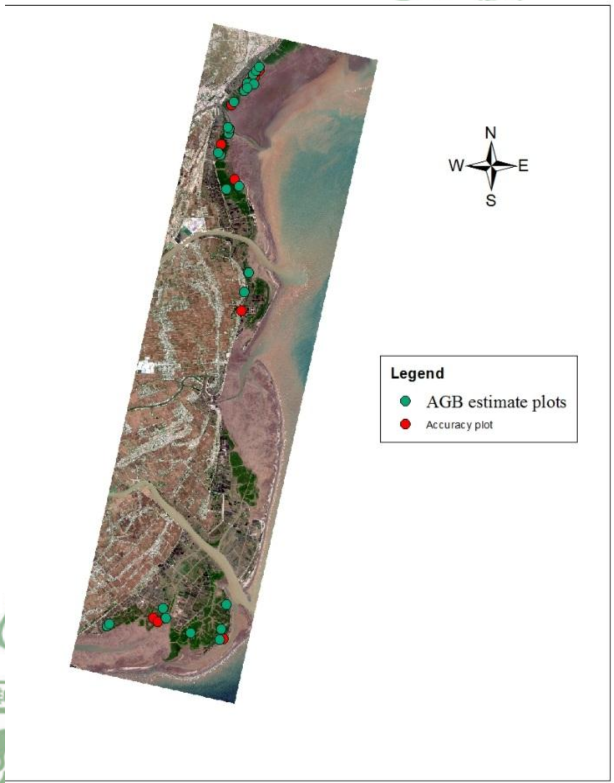

Figure 3: Sampling location

3.3 Data analysis

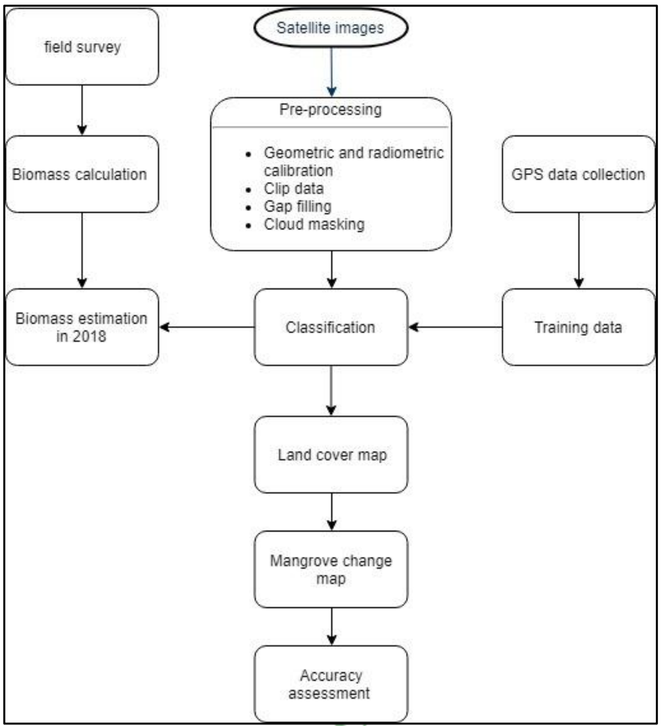

Figure 4: Diagram of Research Workflow

3.3.1 Image pre-processing

All of Landsat data were used pre-processing to allow inter comparison between data, to normalize the data, to correct the atmospheric effects, and to reduce noise. The analyses included radiometric calibration, the creation of multispectral data, subsetting analysis, gap-filling analysis, and cloud masking. The pre-processing analysis were used in this study are explained below:

3.3.1.1 Radiometric Calibration of Satellite

Atmospheric correction are required to remove the scattering absorption effects from the atmosphere to obtain the surface reflectance characterizing and then create image data for classification and monitoring earth surface. (Song, Woodcock, Seto, Lenney, & Macomber, 2001).

The brightness value measured for any object will be influenced by the factor asscene illumination, atmospheric conditions, instrument response characteristics, and viewing geometry. However, we can repair that factor by some tool or application though the below two step:

Fist, Landsat Calibration was used to convert Landsat TM, and ETM+ digital numbers to spectral radiance or exoatmospheric reflectance (reflectance above the atmosphere) using published post launch gains and offsets.

$$L_\lambda = LMIN_\lambda + \left(\frac{LMAX_\lambda - LMIN_\lambda}{QCALMAX - QCALMIN}\right)(QCALMAX - QCALMIN)$$

The spectral radiance (L_λ) is calculated using the following equation:

Where:

- QCAL is the calibrated and quantized scaled radiance in units of digital

Numbers

- $LMIN_\lambda$ is the spectral radiance that is scaled to QCALMIN in watts/(meter squared*ster*µm)
- $LMAX_\lambda$ is the spectral radiance that is scaled to QCALMAXin watts/(meter squared*ster*µm)
- QCALMIN is the minimum quantized calibrated pixel value in Digital Numbers
- QCALMAX is the maximum quantized calibrated pixel value in Digital Numbers

The second step involved calculating top of atmosphere (TOA) reflectance for each band. This calibration were used for illumination variations (sun angle and Earth-sun distance). Calibration is applied base on pixel by pixel for each sense (Chavez Jr, 1989). The TOA reflectance of the Earth is computed according to the equation:

$$\boldsymbol{p_\lambda \frac{\pi * L_\lambda * d^2}{ESUN_\lambda * \cos\theta_s}}$$

Where:

ρλ= Planetary TOA reflectance [unitless]

π= Mathematical constant equal to ~3.14159 [unitless]

Lλ= Spectral radiance at the sensor's aperture [W/(m2 sr µm)]

d= Earth–Sun distance [astronomical units]

ESUNλ= Mean exoatmospheric solar irradiance [W/(m2 μm)]

θs= Solar zenith angle [degrees]

3.3.2 Filling the Gaps of Landsat 7 ETM+ image.

On May 31, 2003, the Scan Line Corrector (SLC), which compensates for the forward motion of Landsat 7, failed. Subsequent efforts to recover the SLC were not successful, and the failure appears to be permanent. Without an operating SLC, the Enhanced Thematic Mapper Plus (ETM+) line of sight now traces a zig-zag pattern along the satellite ground track. As a result, imaged area is duplicated, with width that increases toward the scene edge.

The Landsat 7 ETM+ is still capable of acquiring useful image data with the SLC turned off, particularly within the central part of any given scene. The Landsat 7 ETM+ therefore continues to acquire image data in the "SLC-off" mode. All Landsat 7 SLC-off data are of the same high radiometric and geometric quality as data collected prior to the SLC failure. An estimated 22 percent of any given scene is lost because of the SLC failure. The maximum width of the data gaps along the edge of the image would be equivalent to one full scan line, or approximately 390 to 450 meters.

Image obtained from Landsat 7 ETM+ image dated October 21th 2003 had scan line errors on the image after acquisition due to sensor malfunction. To fix this problem "Gapes Filling tool in ENVI 5.3" software was used. This tool works with the standard Level 1 terrain corrected (L1T) GeoTIFF format images obtained from Landsat. The gap fill procedure works by using two sources of images as input data which is one working image and two reference images (usgs.gov, c2018).

Multiple SLC-off images are required to utilize this method. Individual bands of each image need to be gap-filled before creating a 3-band image. For instance, in order to gap-fill Image 1 with Image 2, a mosaic will need to be made of Band 1 from Image 1 and Image 2 together. The bands can then be stacked to create the RGB image. Gap filling process by using ENVI 5.3 will describe in below:

- Open ENVI 5.3
- Open the .tif band files to be used.
- Select Map -> Mosaicking -> Georeferenced

- Select Import -> Import Files and Edit Properties. Click Open to choose the files you want to gap-fill; they will populate the left-hand frame.
- Highlight one file and click OK, setting the Background See Through-Data Value to Ignore to 0. Colour balancing can be done to adjust any brightness differences between the images, if needed.
- Repeat for all files
- Select File -> Apply, and assign an output file name and select other applicable options.
- Click OK.

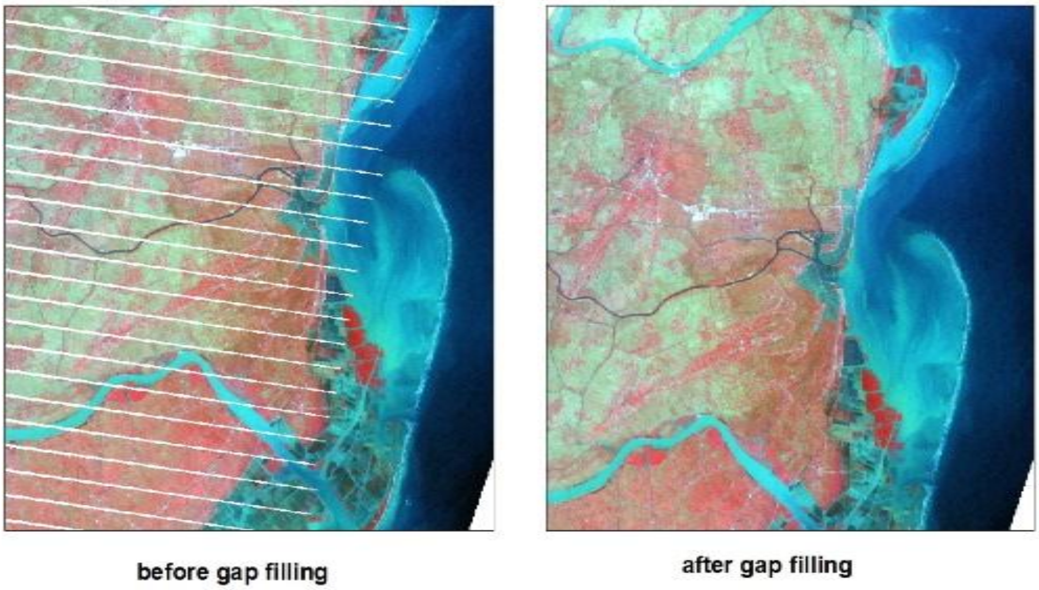

Figure 5: Landsat 7 Image (Band 4, 3, 2) Received On October 21th 2003 before and After Gap Filling

3.3.3 Cloud Masking

Cloud and cloud shadow are common feature of visible and near infrared satellite image in the world especially in tropical and subtropical (Martinuzzi, Gould, & González, 2007). Masking of cloud and cloud shadow is an important step for mapping of land surface attributes. Cloud and cloud shadow is particularly a problem for land cover change analysis, because cloud may be mapped as false changes, and the changing can be more than actual changes this lead to reduce accuracy of land cover map (Huang et al., 2010).The limitation was that researcher unable to replace the masked areas with pixels from corresponding cloud-free image. Thus, mosaicking tool in ENVI 5.3 was used for automated placement of georeferenced images within a georeferenced output mosaic. The purpose of this analysis was to confine and remove the remaining cloud and cloud shadow cover area. The remaining cloud cover was identified using the image interpretation by true colour image using band combination red, blue and green (RGB). Cloud area was identified by white colour, and then compare them with a clear image to verify write the features either to be cloud or non-cloud area.

3.4 Classification

Classification can be considered as the process of pattern recognition or identification of the pattern associated with each pixel position in an image in terms of the characteristics of the objects or materials those are present at the corresponding point on the earth's surface (Syed et al., 2001). The multispectral subset data of the multi-temporal Landsat series (TM, ETM+ SLC-off, SLC-off gap-filled, and OLI_TIRS) were then analysed for classification analysis.

The supervised classification techniques were applied in this study. Classification was carried out on the Landsat imagery to determine the land use land cover. The composite bands used represented false colour combination.

3.4.1 Supervised classification

Supervised classification methods require input from an analyst. The input from analyst is known as training set. Training sample is the most important factor in the supervised satellite image classification methods. Accuracy of the methods highly depends on the samples taken for training. Training samples are two types, one used for classification and another for supervising classification accuracy. Supervised classification includes additional functionality such as analysing input data, creating training samples and signature files, and determining the quality of the training samples and signature files (Abburu & Golla, 2015).

3.4.1.1 Maximum likelihood supervised classifier

Maximum Likelihood is a supervised classifier popularly used in remote sensing image classification. It considers the variance and covariance of class signatures to assign each object or pixel to a class (Sisodia, Tiwari, & Kumar, 2014). Classification in this study by maximum likelihood supervised classifier was showed in below:

- Step 1: Display the three-band overlay composite image. The visible channel, the channel are associated with red, green and blue, respectively so that the clouds look white, vegetation looks green, water looks dark and lands without vegetation looks different shades of brown. After that, we take a careful look at the available features and determine the set of classes into which the image is to be segmented.

- Step 2: Using 'box-cursor' to choose representative training samples for each of the desired classes from the colour composite image. These pixels are said to form training data. Based on the data picked from the study area, a set of training areas were depicted as polygon shape files storing the identity for each land cover type in a column in the attribute table (see Table 6).

- Step 3: Using the trained classifier to classify every pixel in the image into one of the desired classes.

-Step 4: Color-encode and show the classified image. Estimate the number of pixels and area for each class and show the statistics for each class.

Based on the condition of study area and the purpose of the research we classify the map into five different land cover type include sparse mangrove, dense Mangrove, agriculture area, water body, other land use (see Table 6).

Table 6: LULC ID and names

ID	LAND COVER CATEGORIES
1	Sparse mangrove
2	Dense Mangrove
3	Agriculture area
4	Water body
5	Other

Some LULC photo from fieldwork:

Figure 6: Open mangrove

Figure 7: Dense mangrove forest

Figure 8: Water body land use

3.5 Accuracy assessment

Accuracy assessment forms the most integral part of the classification process. No classification is complete until its accuracy has been assessed. Classification remains a pretty picture without an accuracy assessment. Accuracy simply denotes the level of agreement between labels assigned by the classifier and the class allocation on the ground collected by the user as the test data. The sample was selected without any biasness. The known reference data was another set of data different from that which is used for the classifier used in the performance of accuracy assessment (Regression).

In this study, 100 ground truth points data (training data) were collected by create random point tool in ArcGIS 10.2. Accuracy assessment was applied by The Error Matrix method and also to determine the kappa of the classification.

3.5.1 The Error Matrix

An error matrix is a square array of numbers set out in rows and columns which express the number of sample units (i.e., pixels, clusters of pixels, and polygons) assigned to a particular category relative to the actual category as verified on the ground. The columns usually represent the reference data while the rows indicate the classification generated from the remotely sensed data (Congalton & Green, 2008).An error matrix is a very effective way to represent accuracy in that the accuracies of each category are plainly described along with both the errors of inclusion (commission errors) and errors of exclusion (omission errors) present in the classification (Congalton, 1991).User's accuracy, producer's accuracy and overall accuracy can be judged with the help of error matrix method. The brief description of the accuracy indexes are given below.

- Overall accuracy

The proportion of the reference pixels which are classified correctly is known as the overall accuracy. It is computed by dividing the total number of correctly classified pixels by the total number reference pixels. It is a very coarse measurement and does not provide the information about the classes that are classified with good accuracy.

$$\textbf{Overall accuracy} = {}^{\boldsymbol{D}}/_{\boldsymbol{N}} * \mathbf{100}$$

Where: D = total number of correct point

N = total number of cell in the error matrix.

- User's accuracy

User's accuracy shows false positives, where pixels are incorrectly classified as a known class when they should have been classified as something else. An example would be where the classified image identifies a pixel as impervious, but the reference identifies it as forest. The impervious class has extra pixels that it should not have according to the reference data. User's accuracy is also referred to as errors of commission, or type 1 error. The data to compute this error rate is read from the rows of the table. The Total row shows the number of points that should have been identified as a given class, according to the reference data (Congalton & Green, 2008).

- Producer's accuracy:

Producer's accuracy is a false negative, where pixels of a known class are classified as something other than that class. An example would be where the classified image identifies a pixel as forest, but it should be actually be impervious. In this case, the impervious class is missing pixels according to the reference data. Producer's accuracy is also referred to as errors of omission, or type 2 error. The data to compute this error rate is read in the columns of the table. The Total column shows the number of points that were identified as a given class, according to the classified map

3.5.2 Kappa Statistics

The Kappa coefficient of agreement is a discrete multivariate analysis technique used to evaluate the accuracy of change detection and classification maps created with remotely sensed imagery. It is calculated from the error matrix and measures the performance of the classification compared with the reference data. The result is the $Kappa_{(hat)}$ statistic which is another method of agreement or accuracy. It includes all elements of the confusion matrix. The $Kappa_{(hat)}$ Statistic is a measure of the difference between the actual agreement between the reference data and an automated classifier and the chance agreement between the reference data and a random classifier. It is calculated as

Kappa = (Observed agreement - Chance agreement)/(1 - Chance agreement)

The statistic serves as an indicator of the extent to which the percentage correct values of an error matrix are due to "True" agreement versus "chance" agreement. As true agreement approaches 1 and chance agreement approaches 0, k approaches 1.The main advantage of using the $Kappa_{(hat)}$ is the ability to use the value as the basis for determining the statistical significance of any given matrix or the differences among matrices

3.6 Estimating Above Ground Biomass

Above-ground biomass can be measured or estimated both destructively and non-destructively. In the destructive method, sometimes also known as the harvest method, the trees are actually cut down and weighed. Sometimes a selected sample of trees are harvested and estimations for the whole population are based on these, especially where there is uniformity in tree size, for example a plantation. The destructive method of biomass estimation is limited to a small area due to the destructive nature, time, expense and labour involved. The non-destructive methods include the estimation based on allometric equations or through remote imagery. Allometric equations have been developed through the use of tree dimensions, such as diameter at breast height (DBH) and tree height, however these are not very useful in heterogeneous forests. Allometric equations are most useful in uniform forests or plantations with similar aged stands (Kumar & Mutanga, 2017).

In recent years, remote sensing was become a great tool support for field survey by avoiding destructive sampling and reducing time and cost for field sampling. Some studies have found strong relationship between spectral reflectance values and biomass within remotely sensed data. After that the truth point ((Anaya, Chuvieco, & Palacios-Orueta, 2009),(Winarso et al., 2017),(Muhd-Ekhzarizal, Mohd-Hasmadi, Hamdan, Mohamad-Roslan, & Noor-Shaila, 2018)).

3.6.1 Allometric Equation

(Anaya et al., 2009)The total AGB was estimated by species-specific allometric equations(Komiyama, Poungparn, & Kato, 2005). Using the Global Wood Density Database density values of oven-dry wood for all species in the mangrove forest in Table 7 (Muhd-Ekhzarizal et al., 2018). All tree species were identified so that the species-specific wood density can be applied for accurate AGB estimation.

The estimation of AGB was based on D and wood density which were measured at the field. The equation for AGB can be expressed as follows:

$$\mathbf{AGB = 0.251\rho \times D^{2.46}}$$

Where: AGB = above ground biomass (kg)

p = wood density (g/cm^3)

D = Diameter at 0.3m with *Rhizophoraceae* species and D = Diameter at breath Height for other species

Source: (Komiyama et al., 2005)

The AGB of *Kandelia candel* species are not include in list of species create by Komiyama (2005). Base on Khan (2005) AGB of K. *candel* can estimate by bellow fomular:

$$AGB = 0.04117(D_{0,1}^{2}H)$$

Where: AGB = aboveground biomass

$D_{0.1}$ = Diameter at 0.1 m of height

H = the total height tree.

Source: (Khan et al., 2005)

Table 7: Wood Density for Each Species in Mangrove Forest According To the Global Wood Density Database

Species	**Vietnamese name**	**Wood density (g cm^{-3})**
Sonneratia caseolaris	Bần	0.390
Rhizophora stylos	Đâng	0.840
Bruguiera gymnorhiza	Vẹt Dù	0.760
Aegiceras corniculatum	Sú	0.510
Kandelia candel	Trang	0.460

Sources: (Zanne et al., 2009)

3.6.2 Vegetation indices and estimate above-ground biomass

A variety of vegetation indices (VIs) have been developed for retrieving vegetation density from optical remote sensing images. The vegetation indices are used to predict the biomass of trees and the most common one is with the normalised difference vegetation index (NDVI) (Li et al., 2007).However using NDVI alone can significantly underestimate the biomass of some woody mangroves because NDVI represents canopy properties rather than trunk properties that are crucial for accurate biomass retrieval (Foody et al., 2001).Consequently, Araujo, (2000)also revealed the same and found that soil-adjusted vegetation index (SAVI) was more promising in characterising biophysical profile of forest (Araujo, dos Santos, & Shimabukuro, 2000). Wicaksono, 2016 also found that the SAVI variable is useful or predicting biomass than NDVI. The reason is that MSAVI reduces the background soil reflectance which is added to vegetation reflectance. (Wicaksono, Danoedoro, Hartono, & Nehren, 2016).

Plot sampling process was implemented to extract Vegetation Index values of the satellite images at the corresponding locations on the ground. The 2018 sentinel 2 image was utilised for this process. A ground plot with the size of 1000 m^2 can cover exactly 10 pixels of 10-m resolution.

3.6.2.1 Normalized Difference Vegetation Index

The sunlight spectrum makes from many different wavelengths. When sunlight strikes objects, certain wavelengths of this spectrum are absorbed and other wavelengths are reflected. NDVI (Normalized Difference Vegetation Index) were used to determine the density of green on a patch of land by observe the distinct colours (wavelengths) of visible and near-infrared sunlight reflected by the plants. NDVI value were calculated on -composite image. band 3 (Red) and 4 (Near Infrared) are used to calculate NDVI in Landsat 7, and band 4 (Red) come with band 5 (Near Infrared) are used for Landsat 8. NDVI is formulated as below

$$\mathbf{NDVI = ((NIR - RED)/(NIR + RED))}$$

Calculations of NDVI for a given pixel always result in a number that ranges from minus one (-1) to plus one (+1); however, no green leaves gives a value close to zero. A zero means no vegetation and close to +1 (0.8 - 0.9) indicates the highest possible density of green leaves (Zaitunah, Ahmad, & Safitri, 2018).

In this study, NDVI was used for classification and estimate biomass of mangrove forest in Thai Binh province.

3.6.2.2 Soil-Adjusted Vegetation Index

In areas where vegetative cover is low (i.e., < 40%) and the soil surface is exposed, the reflectance of light in the red and near-infrared spectra can influence vegetation index values. This is especially problematic when comparisons are being made across different soil types that may reflect different amounts of light in the red and near infrared wavelengths (i.e., soils with different brightness values). The soil-adjusted vegetation index was developed as a modification of the Normalized

Difference Vegetation Index to correct for the influence of soil brightness when vegetative cover is low. The SAVI is structured similar to the NDVI but with the addition of a “soil brightness correction factor (L)”

$$\textbf{SAVI} = \frac{P_{NIR} - P_{Red}}{P_{NIR} + P_{Red} + L}\,\textbf{(L+1)}$$ (Huete, 1988)

Where: P_{NIR} is the reflectance value of the near infrared band

P_{Red} is reflectance of the red band

L is the soil brightness correction factor.

The value of L varies by the amount or cover of green vegetation: in very high vegetation regions, L=0; and in areas with no green vegetation, L=1. Generally, an L=0.5 works well in most situations and is the default value used. In this study, soil brightness correction factor (L) was used L = 0.5.

3.6.2.3 Green Normalized Difference Vegetation Index

Green Normalized Difference Vegetation Index (GNDVI) is modified version of NDVI to be more sensitive to the variation of chlorophyll content in the forest. “The highest correlation values with leaf N content and DM were obtained with the GNDVI index in all data acquisition periods and both experimental phases. … GNDVI was more sensible than NDVI to identify different concentration rates of chlorophyll, which is highly correlated at nitrogen, in two species of plants”. GNDVI uses visible green (instead of visible red) and near infrared. Use of the visible green band extends sensitivity of index across this higher Chlorophyll concentration range. Useful index for measuring rates of photosynthesis and monitoring plant stress (Gitelson, Kaufman, & Merzlyak, 1996)

GNDVI = (NIR – green)/(NIR + green) (Gitelson et al., 1996)

Where: GNDVI = Green Normalized Difference Vegetation Index

NIR: is the reflectance value of the near infrared band

Green: is reflectance of the green band

3.6.2.4 Global Environmental Monitoring Index

GEMI (Global Environment Monitoring Index) complies better to the requirements expressed above than NDVI, over the entire range of vegetation values, and for all atmospheric conditions. It is seen that, when the atmospheric optical thickness increases from clear to more turbid conditions, the range of 'transmission' of NDVI is larger than that of GEMI. Additional studies, to be reported on elsewhere, have shown that the biological information content of this index is at least as good as that of the NDVI (Pinty & Verstraete, 1992).

$$\mathbf{GEMI} = \boldsymbol{n} * (\mathbf{1} - \mathbf{0.25}\boldsymbol{n}) - \frac{\boldsymbol{RED} - 0.125}{1 - \boldsymbol{RED}}$$

Where:

$$\mathbf{n} = \frac{2(\boldsymbol{NIR}^2 - \boldsymbol{Red}^2) + 1.5\boldsymbol{NIR} + 0.5\boldsymbol{Red}}{\boldsymbol{NIR} + \boldsymbol{Red} + 0.5}$$

NIR = pixel values from the near infrared band

Red = pixel values from the red band

3.7 Regression analysis

Regression models are some of the main techniques used to predict AGB apart from K nearest neighbourhood and neural network (Lu, 2006). A relationship between one dependent variable and one or more independent variables can be identified using regression analysis. The two commonly used regression models are, simple linear and multiple linear regression models (Quinn & Keough, 2002).

3.7.1 Linear regression

Researchers widely use linear regression model because the model describes the linear relationship between independent (x) and dependent (y) variables. It defines variation in y with a change in x and a new y value can be predicted from a new value of x (Quinn & Keough, 2002). In linear regression analysis, AGB was used as the dependent variable and NDVI, SAVI, GNDVI, GEMI were used as the independent variable to determine the change in the AGB. The coefficient of determination (R^2)

was obtained to check the variability of vegetation indices can be caused or explained by its relationship to above ground biomass (Tang & Mayersohn, 2007).

A total of 37 plots observed in the field were used for model development and validation.

Linear regression function:

$$Y = \beta_0 + \beta_1 * X$$

Where: Y is the predicted biomass

$\beta 0$ and $\beta 1$ are model coefficients

X is vegetation indices value

3.7.2 Model validation and accuracy assessment

A validity check is performed to measure the prediction accuracy. Thus, validation process is essential before any model can be used. The predicted AGB obtained from the model was correlated with the calculated AGB to observe the coefficient of determination (R^2) of model validation. Furthermore, the Root Mean Square Error (RMSE) was calculated using below formula:

Root Mean Square Error calculation:

$$\textbf{RMSE} = \sqrt{\frac{\sum_{i=1}^{n}(\hat{y}-Y)^2}{n}}$$

Where:

RMSE is Root Mean Square Error

Y is biomass observed or calculated using allometric equation

$\hat{y}$ is biomass predicted or derived from the radar backscatter using the model

n is the number of validating plots.

CHAPTER 4: RESULT AND DISCUSSION

4.1 Mangrove Classification

4.1.1 Classification feature

Table 8 shows five classes in each of the classes obtained were assigned a class name and class colour to reflect the true nature of objects as they appeared on the ground. Colours assigned reflected the suspected areas of mangrove forests, water body, and agriculture area. There colours remain constant for all classified image and labelled the same colour to avoid confusion when doing accuracy check (Table 8).

Table 8: Class Name and Assigned Class Colours

Value	Land cover	Color
1	Open mangrove	
2	Dense Mangrove	
3	Agriculture area	
4	Water body	
5	Other	

Based on the classification above, it can be identified that the elements in the area change map have color representation in several classes, namely open mangrove, dense mangrove, agriculture area, water body and other. Open mangrove is mangrove forest with low density <1000 tree / ha (Herison, Yulianda, Kusmana, Nurjaya, & Adrianto, 2014) or the new planting forest area. Dense mangrove is dense of mangrove vegetation constraint the coastal area in the various diameter of tree. Unlike the mangrove forest, in this study also identified the type of land use for agriculture. Agriculture is land covered with temporary crops followed by harvest period, crop fields and pastures and other type of cultivation. Water bodies are areas that are sources of water such as stream, lakes, rivers, seas and so on. The mapping results in this study identified sea and watery areas that are scattered in several areas. And then Other land cover which is another area of use, which is the use of areas in various purposes such as residence, sediment area, construction and etc.

In order to mapping land use changing in Thai Binh coastal zone, so the classified needed to do especially for mangrove forest. Most applications related to mangrove mapping usually focus on the discrete differentiation between mangrove and non-mangrove areas or on the qualitative assessment of species, growth status, or condition to derive classes such as “dense” or “sparse” mangrove forests (Q. T. Vo, Oppelt, Leinenkugel, & Kuenzer, 2013). In any case, grouping shows the values for each land characteristic. This was obtained through the results of map observations and literature studies. Furthermore, each value will be used consistently in the analysis process to identify changes in land cover.

4.1.2 Mangrove Classification mapping

In this study, supervised classification (maximum likelihood method) was performed with the help of training site obtained from the field. Five land cover classes were identified include dense mangrove, Open mangrove, water body, rice field, and other land use the result in Figure 9 Shows the various LULC. The classified satellite image of the year 1998 and 2018 shows a significant change in land use/land cover in the study area.

Each of the land use and land cover map was compared to the reference data to assess the accuracy of the classification. The reference data were prepared by considering sample points (collecting by GPS), the field knowledge and Google earth. During the field visits a hand held GPS (Global Positioning System) is used to identify the exact position of the place under consideration with latitude and longitude and its type by visual observation. The ground truth data so obtained was used to verify the classification accuracy.

We considered five images taken at approximately equidistant time points (1998, 2003, 2008, 2013, and 2018) over the study period. By comparing classified images from two adjacent time points, the areas mangroves changed was identified. The study area covers an area of 55201.86ha. In 1998, about 4508.73ha representing 8.17% of the total area covered by open mangrove increased to 4563.45ha in the year 2003 (occupying 8.27% of the study area). In the year 2007 the area of open mangrove are 3230.28 ha that is 8.27%. In 2013, this mangrove was increased to 4511.07 ha equivalent to 7.88%. However, it was slight decrease in 2018 it just 4148.83 ha or

7.51%.

Figure 9 shows dense mangrove class in the study area between 1998 and 2018, Thai Binh province gained 1072.85ha dense mangrove forest. If we assume equal yearly increase, this would mean an increase of 53.64ha per year between 1998 and 2018. The dense mangrove area slight increased from 1366.2 ha in 1998 to 1372.32ha in 2003 and sight decreased to 1203.57ha in 2007, in 2013 it increased to 1834.02ha and significant increase in 2018 (2439.05ha). Regarding proportions, mangroves have been found statistically increased 0.45%, decreased 12.30%, and increased 52.38% and increased 32.99% between 1998 and 2003, 2007, 2013 and from 2013 to 2018 respectively (Table 10).

This study indicated that mangrove forest area was increase from 1998 to 2018. The open mangrove was decreased 359.9ha but dense mangrove increased 1072.85ha. The result from Dat, (2011) showed that mangrove forest in Thai Binh province increased 987ha from 1990 to 2007. If we assume equal yearly increase, this would mean an increase of 58.06 ha per year. The increasing of mangrove area is higher than our study 22.41ha per year (Dat & Yoshino, 2011). Although mangrove area was increasing in study area but it was decreasing in the in the Northern coast of Vietnam because the decline of mangrove in Quang Ninh and Hai Phong province (Dat & Yoshino, 2011).

There are two main reason for the increasing of mangrove forest area in Thai Binh province. (1) A large number of project were implemented in Thai Binh province. In 2006, a project were implemented by Asian Forest Cooperation Organization about afforest, rehabilitate and sustainably manage mangrove forest ecosystems; raise awareness and enhance the knowledge and capacities of local communities on the rehabilitation, protection and sustainable development of mangrove forests, biodiversity conservation, climate change mitigation and livelihood improvement strategies. In the same this year, International Federation of Red Cross and Red Crescent Societies (IFRC) and Japanese Red Cross (JRC) was implemented a project for added mangrove trees in mangrove forests established in earlier phases and expanded its planting of bamboo along river dykes and along coastal and river bank stretches. The aim of the planting component was to better protect dykes and communities from hazards such as typhoons, storms and floods (VNRC, 2006). (2) The natural development of mangrove forest.

Natural regeneration of seedlings in mangrove forest is an important part of the secondary succession process. The growth of natural types of mangrove seedlings has a relationship with the availability of mother trees that have spread seeds to mangrove areas. Furthermore, the success of mangrove vegetation growth can be influenced by several factors, namely the environmental parameters of the water in the form of pH, COD, BOD and TSS that are still on the tolerant threshold for the mangrove vegetation produced from planting or natural. In fact, the soil fertility level around mangrove habitat in the front zone is low (Wallacea, 2016). This is due to the higher tidal frequency and flooding, which results in frequent washing of nutrients contrast based on research (Salmo, Lovelock, & Duke, 2013) shows that the trend of increasing new soil fertility will be seen in observations in the rehabilitation area in a long time span.

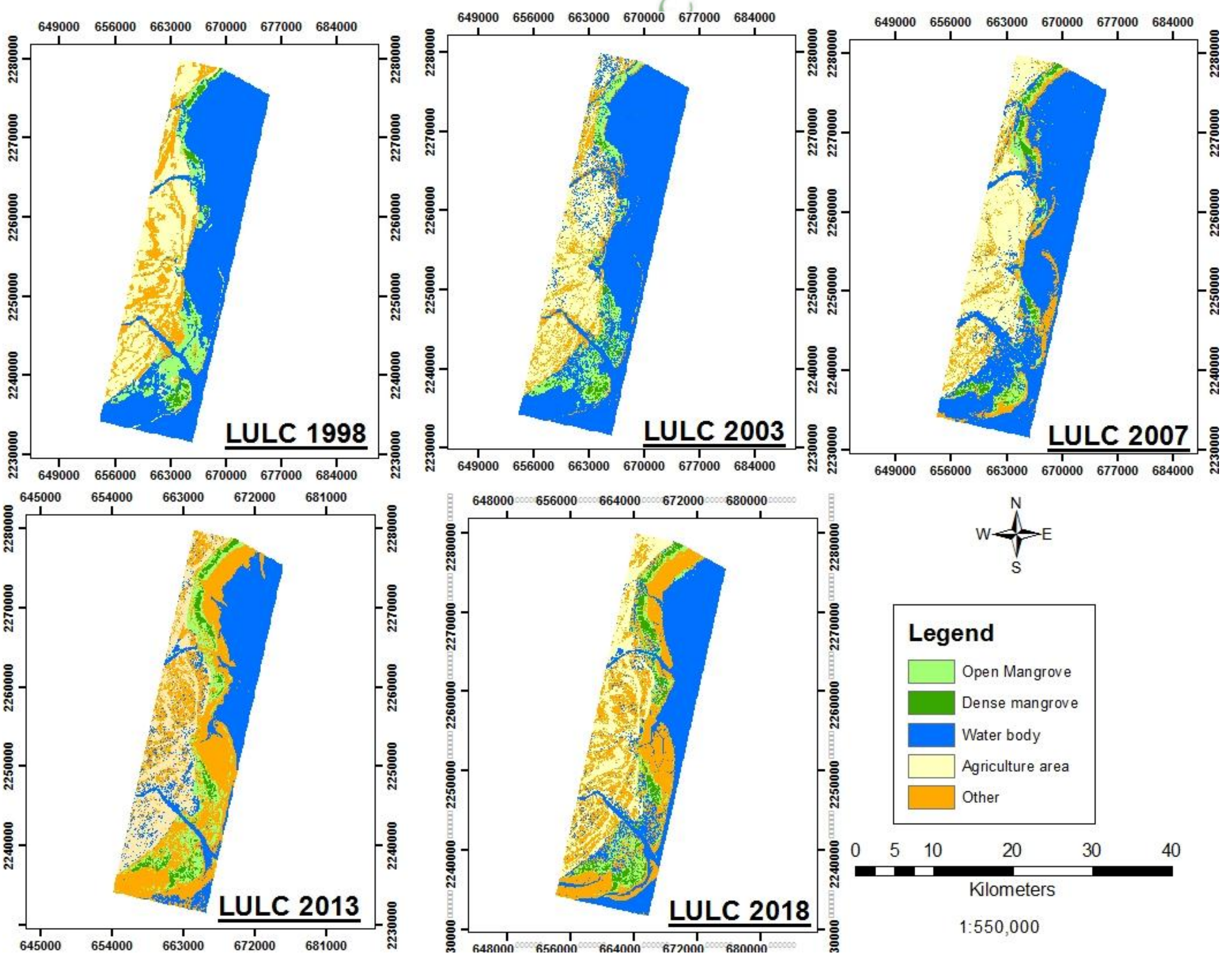

Figure 9: Land Use Land Cover Map in 1998, 2003, 2007, 2013, 2018

Table 9: Area of LULC for Years 1998, 2003, 2007, 2013, 2018

	Open mangrove (ha)	Dense mangrove (ha)	Water (ha)	Agriculture area (ha)	Other (ha)
1998	4508.73	1366.20	29783.07	12119.30	7400.52
2003	4563.45	1372.32	31008.60	11910.60	6355.17
2007	3230.28	1203.57	28746.09	13969.44	8060.85
2013	4511.07	1834.02	26089.20	11636.91	13208.85
2018	4148.83	2439.05	18913.04	7859.42	21849.95

Table 10: Percent (%) of Land Cover in Study Area

Land cover	1998	2003	2007	2013	2018
Open mangrove	8.17	2.48	53.98	21.96	13.41
Dense mangrove	8.27	2.49	56.16	21.57	11.51
Water	5.85	2.18	52.07	25.30	14.60
Agriculture area	7.88	3.20	45.55	20.32	23.06
Other	7.51	4.42	34.26	14.24	39.58

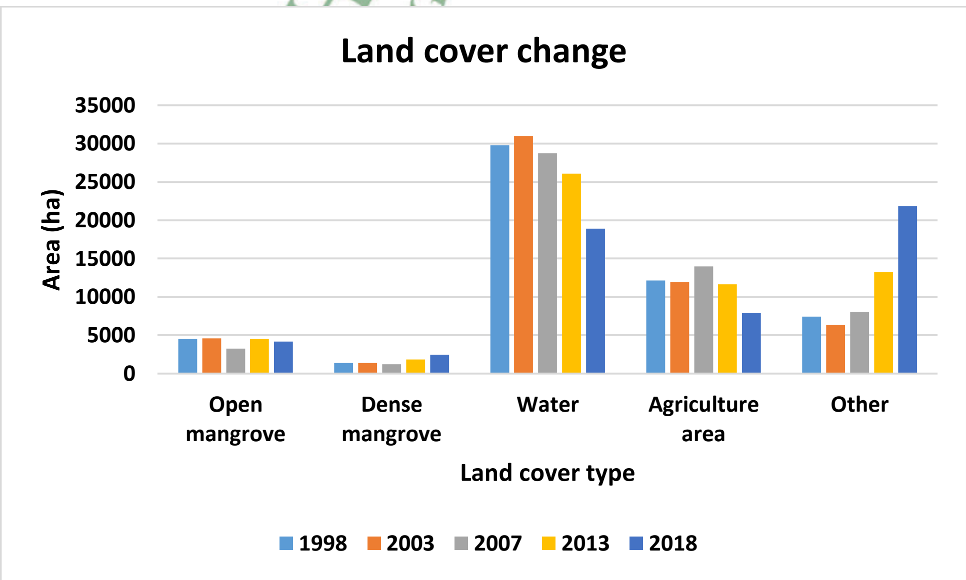

Figure 10: Land cover change from 1998 to 2018

Although the area of water body was increased from 1998 to 2003 but it decreased from 2003 to 2018. In 1998, the extent of water was 50.79% that is

28073.07ha. In 2003, the extent is 56.16% that is 31008.6 ha. In 2007, it decreased to 28746.09ha (52.07%). In 2013, the water body area was 26089.2 ha that is 45.55%. In 2018, water surface was decreased significantly to 18913.04 (34.26%).Changes in Water body can be attributed to the twice - daily inundation of water in mangrove areas. This results in the overflow of the river causing the marshy ground and lots of water on the surface of the ground. As a result, Water body tends to increase or decrease depending on the day and time of capture (Yevugah, 2017).

Agriculture area reduced 208.7 ha from 12119.3ha in 1998 to 11910.6ha in 2003, however, increased by 2058.8ha from 2003 to 2007, while decreased by 2332.53ha from 2007 to 2013, following a decline of 3777.49 ha from 2013 to 2018. In generally, the agriculture area are not significant changing. Their value around 12000 ha in 1998, 2003, 2013, and they was increased to 13969ha in 2007 and decreased to 11636ha in 2018. The agriculture area was effected by the urbanization of Thai Binh province (Van Suu, 2009).

Other land used like sediment area, construction area, bare land were group into a group of land use with the name is other land used. Sediment area which is a part of other land use are Located in the area of tidal influence, therefore other land used was change two time per day base on the tide activity. In 1998, the area of other land use were 7400.52ha that is 13.39%. This area was decreased in 2003 6355.17ha (11.51%). In 2007, this area increased 1705.68ha and they are keep increased to 13208.85ha in 2013. In 2018 other land used significantly increased to 21849.95 that is 39.58% in total study area.

4.1.3 Land use land cover change Accuracy Assessment

The classified images have been evaluated quantitatively through accuracy assessment of all the land cover classes. Producer’s accuracy is the measure of how accurately a class can be classified in an image. It is the percentage of pixels that should have been put in a given class but they are not. User’s accuracy simply implies the confidence of the class in a classified image. Producer’s accuracy is the overall accuracy of the classified image. It simply indicates the pixels that were placed in a given class when they actually belong to another class. In accuracy table (Table 11,

Table 13, Table 12, Table 14, Table 15) the values represent points. The columns represent the actual values, and the rows represent the classified values

4.1.3.1 Accuracy Assessment of the Classified Images in 1998

From the accuracy table (Table 11), it has been shown that the overall accuracy of classification image in year 1998 are 93%. The overall Kappa statistic are 0.88 in year 2000 classified image. The lowest producer's accuracy is sparse mangrove; the highest are dense mangrove and agriculture area 100% accuracy. For user's accuracy, the lowest accuracy is Agriculture area (85.7%) and the highest accuracy is dense mangrove (100%)

Table 11: Accuracy Assessment of the Classified Images in 1998.

Actual / Predicted	Open mangrove	Dense mangrove	Water body	Agriculture area	Other	Total	User's accuracy
Sparse mangrove	9	0	1	0	0	10	90.00
Dense mangrove	0	4	0	0	0	4	100.00
Water body	1	0	54	0	1	56	96.43
Agriculture area	0	0	1	18	2	21	85.71
Other	1	0	0	0	8	9	88.89
total	11	4	56	18	11	100	
Producer's accuracy	81.82	100.00	96.43	100.00	72.73		
Overall accuracy = 93%				Overall Kappa = 0.88			

4.1.3.2 Accuracy Assessment of the Classified Images in 2007

The accuracy assessment based on Error matrix method had given in Table 12. The overall classification accuracy based on error matrix method is 96%, Kappa statistics is 0.93. The user's accuracy no lower than 91.67%. There are two class in producer's accuracy are lower than 100% are sparse mangrove (66.67%) and other land (86.67%).

Table 12: Accuracy Assessment of the Classified Images in 2007

Actual / Predicted	Open mangrove	Dense mangrove	Water body	Agriculture area	Other	total	User's accuracy
Open mangrove	4	0	0	0	0	4	100.00
Dense mangrove	0	3	0	0	0	3	100.00
Water body	2	0	54	0	0	56	96.43
Agriculture area	0	0	0	22	2	24	91.67
Other	0	0	0	0	13	13	100.00
total	6	3	54	22	15	100	
Producer's accuracy	66.67	100.00	100.00	100.00	86.67		
Overall accuracy = 96%				Overall Kappa = 0.93			

4.1.3.3 Accuracy Assessment of the Classified Images in 2003

In classified image year 2003, the overall accuracy is 86%, that accuracy is lower than year 1998. The Overall Kappa statistic are 0.79

Table 13: Accuracy Assessment of the Classified Images in 2003

Actual / Predicted	Sparse mangrove	Dense mangrove	Water body	Agriculture area	Other	total	User's accuracy
Open mangrove	12	0	4	0	0	16	75.00
Dense mangrove	2	2	0	0	0	4	50.00
Water body	3	0	43	1	0	47	91.49
Agriculture area	0	0	0	22	3	25	88.00
Other	1	0	0	0	7	8	87.50
Total	18	2	47	23	10	100	
Producers accuracy	66.67	100.00	91.49	95.65	70.00		
Overall accuracy = 86%				Overall Kappa = 0.79			

4.1.3.4 Accuracy Assessment of the Classified Images in 2013

The overall accuracy of classified image year 2013 is 94% and overall Kappa statistic is 0.91. The producer's accuracy and user's accuracy of every classified are higher than 80%.

Table 14: Accuracy Assessment of the Classified Images in 2013

Actual / Predicted	Sparse mangrove	Dense mangrove	Water body	Agriculture area	Other	Total	User's accuracy
Open mangrove	8	0	0	1	0	9	88.89
Dense mangrove	0	4	0	0	0	4	100.00
Water body	2	0	48	0	0	50	96.00
Agriculture area	0	0	0	21	2	23	91.30
Other	0	1	0	0	13	14	92.86
total	10	5	48	22	15	100	
Producers accuracy	80.00	80.00	100.00	95.45	86.67		
Overall accuracy = 94%				Overall Kappa = 0.91			

4.1.3.5 Accuracy Assessment of the Classified Images in 2018

In classified images year 2018, the overall accuracy is 91% and the overall Kappa statistic is 0.87. The lowest user's accuracy is dense forest classified (71.43%); the highest accuracy is open forest (100%). The producer's accuracy of dense forest is same value with the user's accuracy. The highest producer's accuracy is water body class (100%)

Table 15: Accuracy Assessment of the Classified Images in 2018

Actual / Predicted	Open mangrove	Dense mangrove	Water body	Agriculture area	Other	Total	User's accuracy
Open mangrove	9	0	0	0	0	9	100.00
Dense mangrove	0	5	0	2	0	7	71.43
Water body	2	0	39	1	0	42	92.86
Agriculture area	0	1	0	23	2	26	88.46
Other	0	1	0	0	15	16	93.75
Total	11	7	39	26	17	100	
Producers accuracy	81.82	71.43	100.00	88.46	88.24		
Overall accuracy = 91%				Overall Kappa = 0.87			

One of the most important final step at classification process is accuracy assessment. The aim of accuracy assessment is to quantitatively assess how effectively the pixels were sampled into the correct land cover classes (Manandhar, Odeh, &

Ancev, 2009). In this research, various statistics related with classification accuracy as well as overall Kappa statistic are computed.

Table 16: Accuracy Assessment overall

Year	Overall Accuracy (%)	Overall Kappa
1998	93	0.88
2003	86	0.79
2007	96	0.93
2013	94	0.91
2018	91	0.87

Table 17: Rating criteria of Kappa statistics

No	Kappa statistics	Strength of agreement
1	<0.00	Poor
2	0.00 - 0.20	Slightly
3	0.21 - 0.40	Fair
4	0.41 - 0.60	Moderate
5	0.61 - 0.80	Substantial
6	0.81 - 1.00	Almost Perfect

Source: (Rwanga & Ndambuki, 2017)

The users of LULC maps need to know how accurate the maps are in order to use the data more correctly and efficiently (Plourde & Congalton, 2003). According to (J. R. Anderson, 1976) the minimum level of interpretation accuracy in the identification of land use and LULC categories from remote sensing data should be at least 85%. It is appropriate with this study that the results from accuracy assessment showed an overall accuracy ranged from 86% - 96% and also the User's accuracy and producer's accuracy ranged have been shown in tables (Table 11, Table 12, Table 13, Table 14, Table 15). Different (LC) classes had differing producer's and user's accuracy levels indicating different levels of omission and commission errors.

Moreover, the Kappa coefficient equal to 1 means perfect agreement where as a value close to zero means that the agreement is no better than would be expected by chance (Rwanga & Ndambuki, 2017). This result showed that there were 4 year (1998, 2007, 2013, and 2018) have >81. It is stated that Kappa values of more than 0.80 indicate good classification performance and only year 2003 was obtained which is rated as substantial. Apart from overall classification accuracy, the above individualized parameters give a classifier a more detailed description of model performance of the particular class or category of his field of interest or study. Since overall accuracy, user's and producer's accuracies, and the Kappa statistics were derived from the error matrices to find the reliability and accuracy of the maps produced in this study.

4.2 Mangrove biomass estimating

For estimations of AGB, we used backscatter characteristics of mangrove forest in Southeast Asia and some researchers ((G. Anderson, Hanson, & Haas, 1993), (Zheng et al., 2004), (Mutanga, Adam, & Cho, 2012)) found empirical functions to estimate AGB, as derived from relationships between vegetation indices and AGB measured on the ground sample plot.

4.2.1 Single linear regression

Conventionally, vegetation indices are utilised as predictors because of the relationship between spectral information catered by optical remote sensing data and vegetation biomass. NDVI, SAVI, GNDVI values of each sampling point locations were extracted from vegetation indices map. Each location were created a buffer zone with radius is 17.8 m or the total buffer area is $1000m^2$. The mean value of NDVI, SAVI, NDVI of the buffer zone was calculate, and ten they were used for developing linear regression models. The derived NDVI, SAVI and GNDVI are illustrated in Figure 17. The scatterplots that have been generated from the linear regression analysis as shown in Figure 11, Figure 12 and Figure 13, indicated the relationship between vegetation indices and measured AGB. Simple linear regression model was developed from the 70% of the data (27 plots) and 30% of plot we was used for check accuracy of model. The correlation between the estimated and observed AGB gave a strong coefficient of determination R^2 are 0.6762 with NDVI, 0.685 with SAVI, 0.672 with green NDVI (see Table 18). The scatter graph of the estimated and observed AGB is presented in Figure 11.

Table 18: Summary of simple linear regression models using single independent variable

No.	Vegetation index	Model	R	R^2	Adjusted R^2
1	NDVI	Y= 148.24x - 40.413	0.822	0.6762	0.667
2	SAVI	Y = 99.093x - 40.7	0.828	0.6851	0.667
3	GNDVI	Y= 231.18x – 60.67	0.820	0.6726	0.677

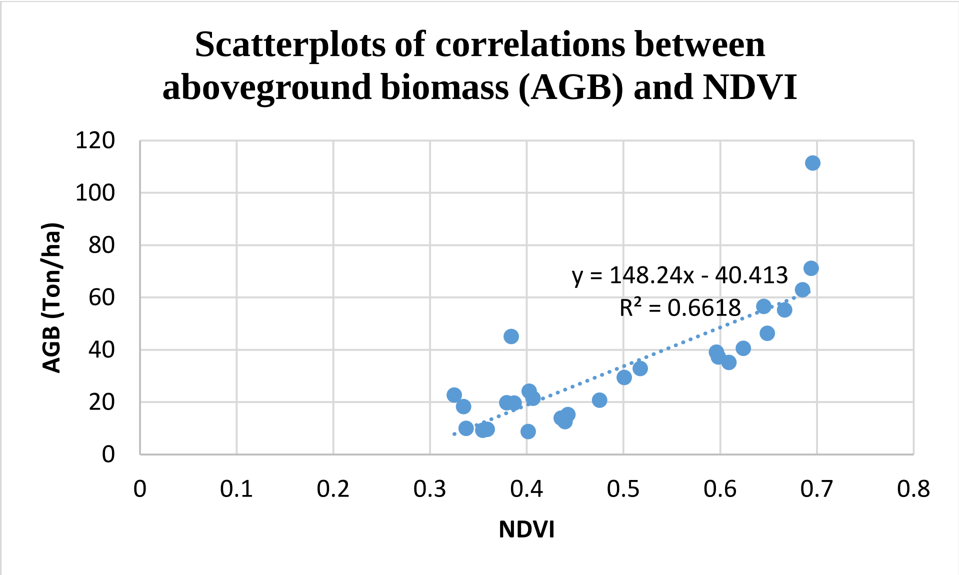

Figure 11: Scatterplots of correlations between aboveground biomass (AGB) and Normalized Difference Vegetation Index (NDVI)

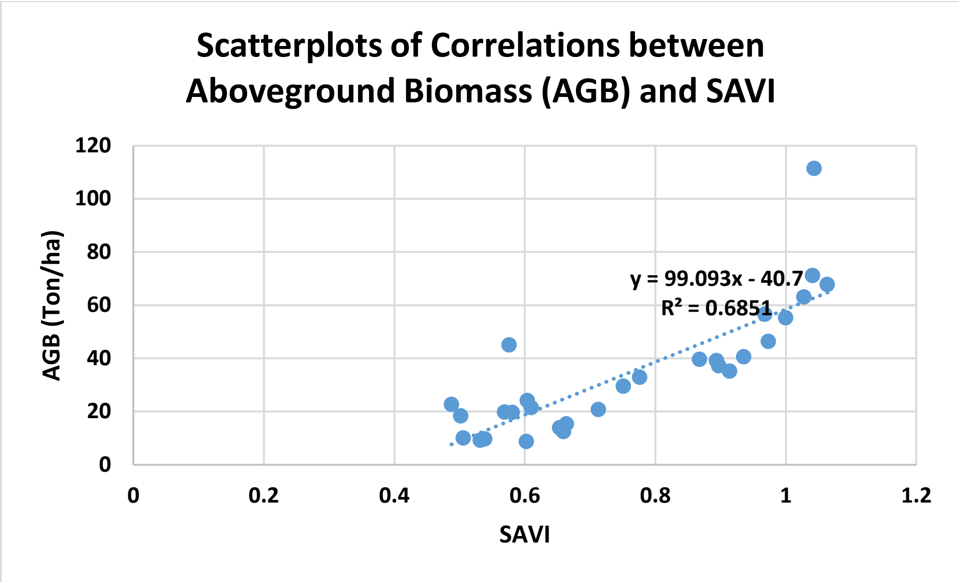

Figure 12: Scatterplots of Correlations between Aboveground Biomass (AGB) and Soil-Adjusted Vegetation Indices (SAVI)

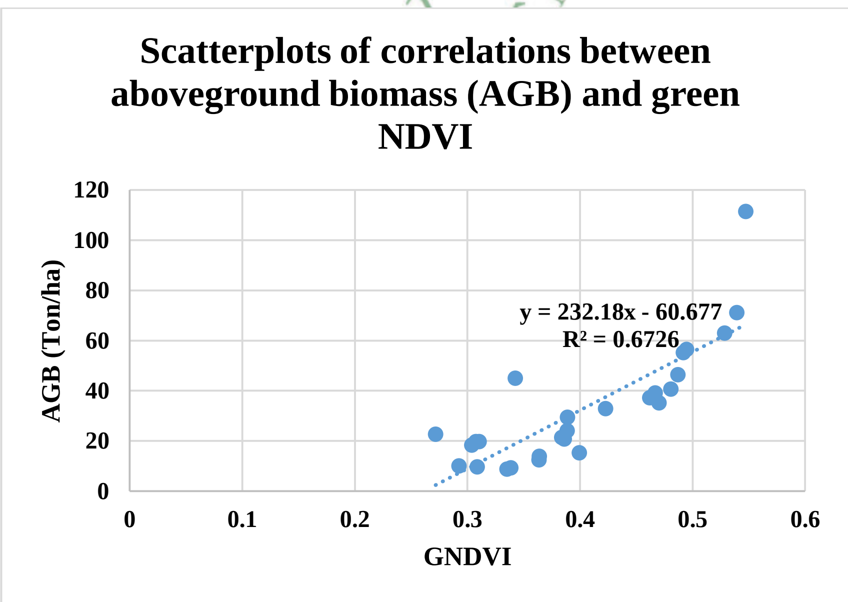

Figure 13: Scatterplots of correlations between aboveground biomass (AGB) and green NDVI (GNDVI)

Coefficient of determination (R^2) is the proportion of the variance in the dependent variable that is predictable from the independent variable. An R^2 of 0 means that dependent variable cannot be predicted from the independent variable and R^2 of 1 mean that dependent variable can be predicted without error from the independent variable (Draper & Smith, 1998). Coefficient of determination of each vegetation index are higher than 0.65 mean that more than 65% is predictable. Thus, AGB can be estimate by the vegetation index NDVI, SAVI, GNDVI.

4.3 AGB Accuracy Assessment

In this study, an independent validation dataset was used for the models accuracy estimation due to the limited number of samples. The model was validated using independent validation plots and the predicted AGB was within agreement with the measured AGB.

Figure 10 shows the linear relationships between the estimated AGB by using single and the field-based measured AGB. The 30% of the dataset (10 plots) was used for model validation to measure the predictive accuracy. The validation dataset was independent of the 70% of the dataset (27 plots) used for developing the model. The root mean square error (RMSE) was calculated based on the validation data (n=10). The result of the RMSE for estimate AGB by NDVI was low with the value of 7.22861 and the simple linear model gave a strong R^2 of 0.92 (see Figure 14).

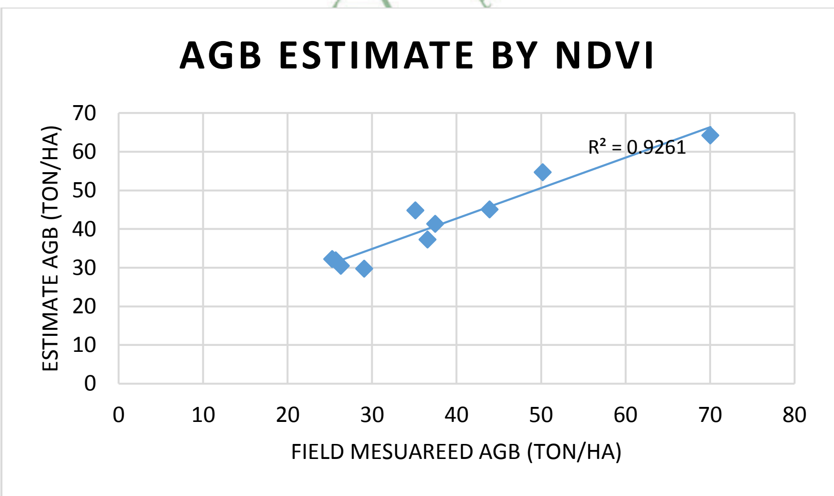

Figure 14: Relationship between NDVI linear regressions to estimated AGB and field-based measured AGB

The root mean square error (RMSE) was calculated based on the validation data (n=10). The result of the RMSE fir estimate AGB by SAVI was low with the value of 7.22897 and the simple linear model gave a strong R² of 0.75.

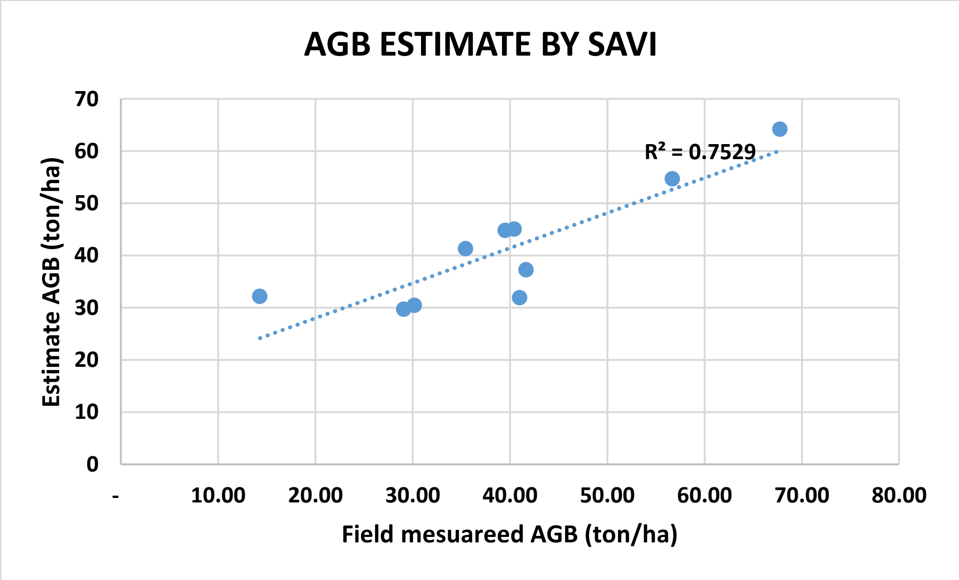

Figure 15: Relationship between SAVI linear regressions to estimated AGB and field-based measured AGB

The root mean square error (RMSE) was calculated based on the validation data (n=10). The result of the RMSE fir estimate AGB by SAVI was low with the value of 7.975 and the simple linear model gave a strong R² of 0.68.

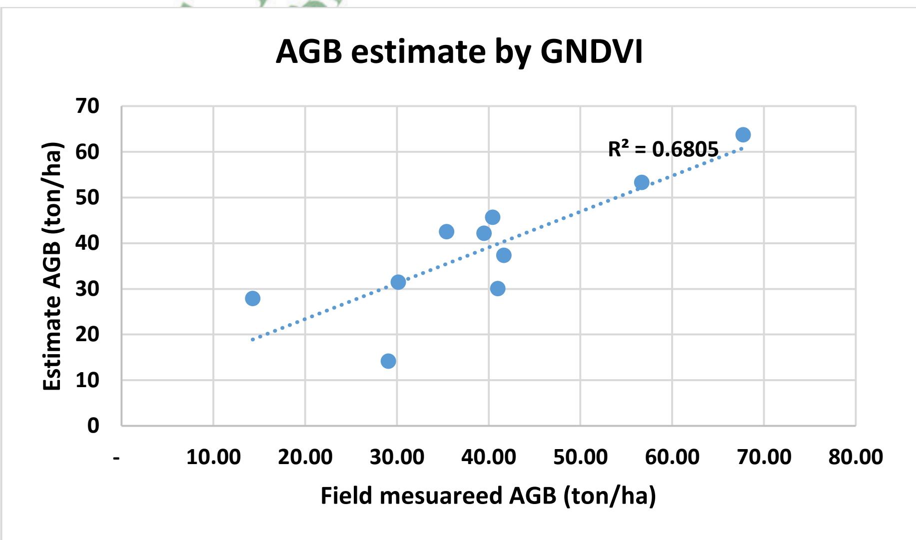

Figure 16: Relationship between GNDVI linear regressions to estimated AGB and field-based measured AGB

In this study the root mean square error (RMSE) are low (no higher than 8) for all of estimated AGB method. It's mean the error of estimate no higher than 8 ton/ha. The study by Goh et al. (2014) found that Study by Goh et al. (2014) found that for estimation of AGB, the RMSE values were between 150 and 152 ton/ha respectively. Thus, the overall RMSE obtained in this present study was acceptable (Goh, Miettinen, Chia, Chew, & Liew, 2014). Using NDVI and SAVI and the similar model, Hamdan et al. (2014a) obtained RMSE = 43.77 ton/ha (r2 = 0.59) and 68.21 ton/ha (r2 = 0.01) respectively (Hamdan, Aziz, & Hasmadi, 2014).

Table 19: AGB accuracy assessment

No.	Vegetation index	R^2	RMSE
1	NDVI	0.9261	7.22861
2	SAVI	0.7529	7.22897
3	GNDVI	0.6805	7.975

In this study, the accuracy of each linear regression models are quite high. Moreover, the highest accuracy is NDVI model with lowest RMSE (7.22861) and highest R^2 (0.9261).

The study was showed that the accuracy is quite high but for the study from Wicaksono (2016) map accuracy make by the model acquired from ALOS AVNIR-2 PC bands is higher than model from vegetation indices. He also indicated that vegetation indices based on visible bands, such as VARI, ARVI, and MSARVI, were not very good in modelling mangrove carbon stock (Wicaksono et al., 2016).

4.4 Spatial Distribution of Mangrove Vegetation Biomass in 1998 and 2018

Aboveground biomass was mapping in this study base on the NDVI, SAVI, GNDVI linear regression model. The AGB was divided into 10 different level (from no biomass to > 80 ton/ha) (see Figure 17).

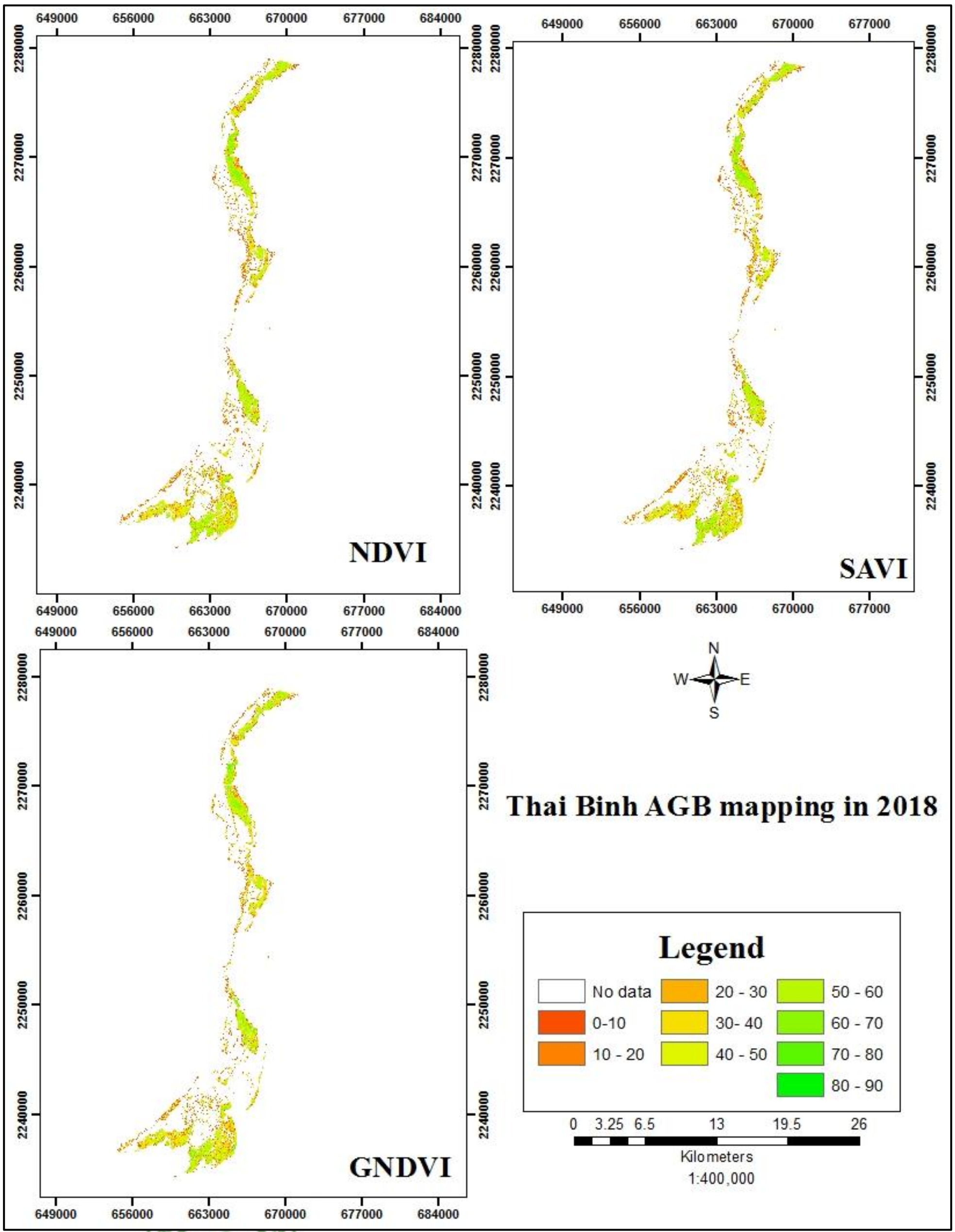

Figure 17: Thai Binh AGB mapping base on vegetation indices in 2018

After build linear regression model for NDVI, SAVI, GNDVI in 2018, we were applied that models for 1998 to estimate the changing in aboveground biomass from 1998 to 2018.

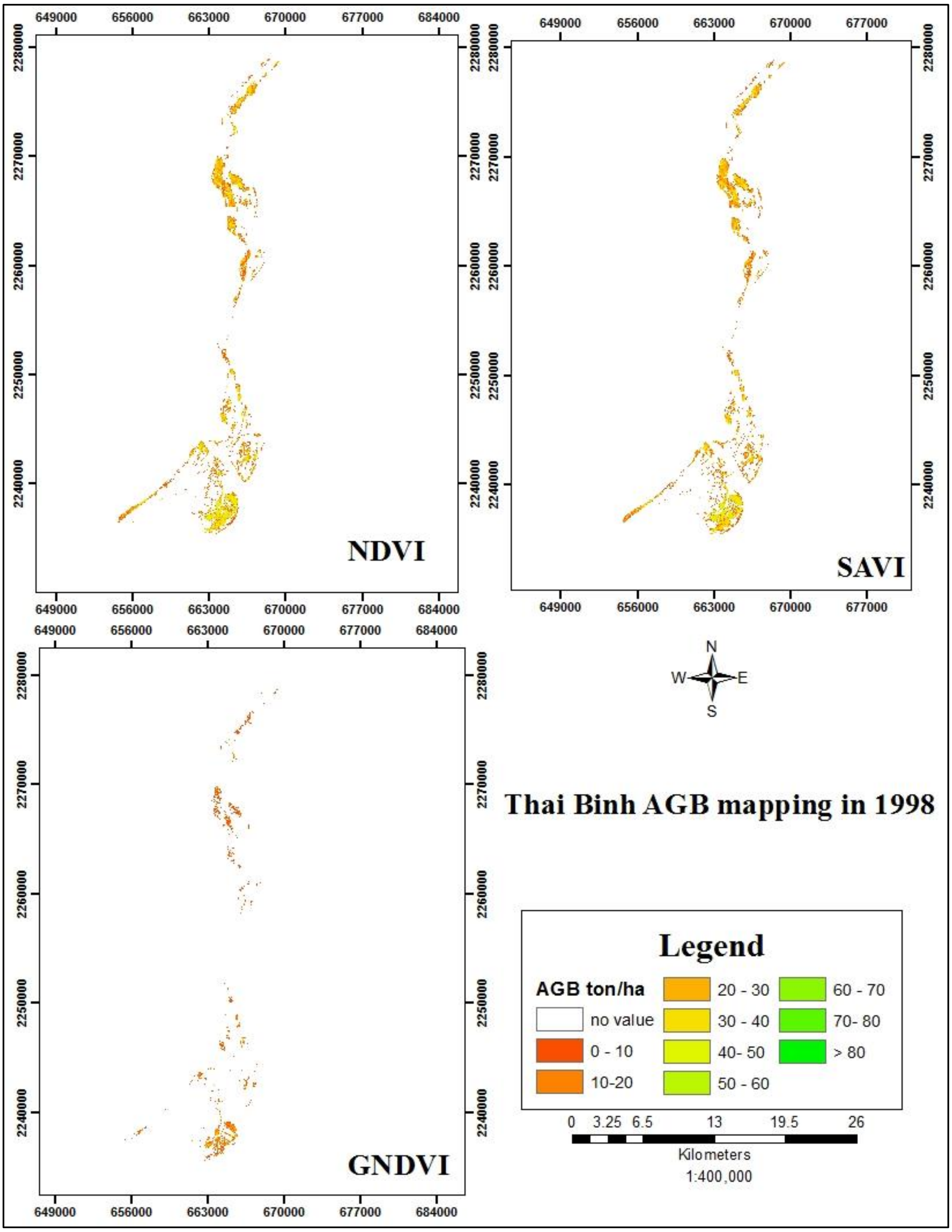

Figure 18: Thai Binh AGB mapping base on vegetation indices in 1998

The results obtained from the AGB in mangroves from 1998 to 2018 are shown in Table 20. The maximum estimated AGB by using NDVI linear regression of 1998 and 2018 are 59.1 t/ha ha-1 and 78.6 ton/ha respectively. The average of AGB in 1998 are 22.569 ton/ha and in 2018 is 37.74 ton/ha. The study from Darmawan (2014) was show that Mangrove AGB in Thai Thuy district Thai Binh province = 13.87 ton/ha, in Thanh An Can Gio 31.61 ton/ha, in Giao thuy district Nam Dinh province is 13.12 ton/ha. (Darmawan et al., 2014). Hanh (2016) showed that the average AGB in Dong Hung commune, Tien Lang district, Hai Phong city are 36.80 ton/ha (Hanh, 2016).

The mangrove AGB in the study area is mainly controlled by the environmental conditions of the mangrove habitat, as in other natural forests. Human activities play an insignificant role in the variation in mangrove AGB since the forest is protected by the Xuan Thuy National Park and replanted by NGO and government program.

Table 20: Table showing estimated AGB by NDVI in 1998 and 2018

Parameter	1998	2018	Total change
Total mangrove AGB of the whole area (ton)	62880	187990	125110
Mean area of mangrove AGB (ton/ha)	22.569	37.745	15.180
Total area (detect by NDVI) (ha)	2786	4980	2194
Maximum AGB (ton/ha)	59.1	78.6	19.5

CHAPTER 5: CONCLUSION, LIMITATION, REMOMENDATION

In this study, the main focus was on assessment of the status of mangrove vegetation and estimate the mangrove biomass in coastal area of Thai Binh province. The research was guided by two propositions, namely; using RS combination with GIS for land cover change detection in the Thai Binh province from 1998 to 2018, and using vegetation indices for estimate mangrove aboveground biomass.

Using RS and GIS, mangrove forest was mapped. The mangrove forest in the Thai Binh province occupied an area of about 5874.93ha in 1998, 5935.77 ha in 2003, 4433.85 ha in 2007, 6345.09ha in 2013 and 6587.88ha in 2018.

5.1 Limitation of the research

There are certain limitations in this research. Absence of high-resolution data for the study area of study area has made it difficult to detect the changing and distribution at the species level. Lack of extensive fieldwork due to time constraints has effect to the accuracy of mangrove forest.

5.2 Recommendation

- This type of study is advisable in the areas where the present rate of degradation and disappearance of mangroves is high and climate change has worsened the situation further. The same study if carried out at different sites would give more clarity to the present work.
- Further research can be carried out if different sensors with different wavelengths can be taken into consideration.
- Assessment of damage of the mangroves at the species level can be carried out with the help of high-resolution remotely sensed imagery.
- Various classification accuracy methods can be tried out to give better classification results.
- Various other vegetation indices or other method to estimate AGB to get better results (Abburu & Golla, 2015).
- Establish more survey plot to get more accuracy in estimate ABG

ACKNOWLEDGEMENT

First and foremost, I would like to give my sincere thanks to my supervisor, Assoc. Prof. Tran Quang Bao, who has accepted me as his master student and offered me so much advice, patiently supervising me and always guiding me in the right direction. I have learned a lot from him. Without his help, I could not have finished my desertion successfully.

I would like to express my gratitude to Institute for Forest Ecology and Environment for they valuable support and collaboration during the sampling in Thai Binh. I also thank to MSc. Nguyen Song Anh and Mr Pham Quang Duong to support me during my fieldwork time.

I would like to thank Mr. Mai Gia Hung in Forest Resources and Environment Centre for support me collected data.

Last but not least, special appreciation to my parents, family members and all of my friend for their constant support that helps me through.

NGUYEN DUC LONG

REFERENCE

Abburu, S., & Golla, S. B. (2015). Satellite image classification methods and techniques: A review. *International journal of computer applications, 119*(8).

AccuWeather. (2018). from https://www.accuweather.com

Adam, E., Mutanga, O., & Rugege, D. (2010). Multispectral and hyperspectral remote sensing for identification and mapping of wetland vegetation: a review. *Wetlands Ecology and Management, 18*(3), 281-296.

Alongi, D. M. (2002). Present state and future of the world's mangrove forests. *Environmental conservation, 29*(3), 331-349.

Anaya, J. A., Chuvieco, E., & Palacios-Orueta, A. (2009). Aboveground biomass assessment in Colombia: A remote sensing approach. *Forest Ecology and Management, 257*(4), 1237-1246.

Anderson, G., Hanson, J., & Haas, R. (1993). Evaluating Landsat Thematic Mapper derived vegetation indices for estimating above-ground biomass on semiarid rangelands. *Remote sensing of Environment, 45*(2), 165-175.

Anderson, J. R. (1976). *A land use and land cover classification system for use with remote sensor data* (Vol. 964): US Government Printing Office.

Araujo, L. S., dos Santos, J. R., & Shimabukuro, Y. E. (2000). relationship between SAVI and biomass data of forest and Savanna Contact Zone in the Brazilian Amazonia. *International Archives of Photogrammetry and Remote Sensing, 33*(B7/1; PART 7), 77-81.

Ball, M. C. (2002). Interactive effects of salinity and irradiance on growth: implications for mangrove forest structure along salinity gradients. *Trees, 16*(2-3), 126-139.

Barsi, J. A., Lee, K., Kvaran, G., Markham, B. L., & Pedelty, J. A. (2014). The spectral response of the Landsat-8 operational land imager. *Remote Sensing, 6*(10), 10232-10251.

Beatley, T., Brower, D., & Schwab, A. K. (2002). *An introduction to coastal zone management*: Island Press.

Beland, M., Goita, K., Bonn, F., & Pham, T. (2006). Assessment of land-cover changes related to shrimp aquaculture using remote sensing data: a case study in the Giao Thuy District, Vietnam. *International Journal of Remote Sensing, 27*(8), 1491-1510.

Blasco, F., Gauquelin, T., Rasolofoharinoro, M., Denis, J., Aizpuru, M., & Caldairou, V. (1998). Recent advances in mangrove studies using remote sensing data. *Marine and Freshwater Research, 49*(4), 287-296.

Brown, S. (1997). *Estimating biomass and biomass change of tropical forests: a primer* (Vol. 134): Food & Agriculture Org.

Cat, V., & Duong, B. (2006). *Assessment of saline water intrusion into estuaries of Red-Thai Binh River during dry season having considered water released from upper reservoirs and tidal fluctuation.* Paper presented at the Proceeding of the Vietnam-Japan Estuary Workshop, Hanoi, Vietnam.

Chander, G., Markham, B. L., & Barsi, J. A. (2007). Revised Landsat-5 thematic mapper radiometric calibration. *IEEE Geoscience and remote sensing letters, 4*(3), 490-494.

Chavez Jr, P. S. (1989). Radiometric calibration of Landsat Thematic Mapper multispectral images. *Photogrammetric engineering and remote sensing, 55*(9), 1285-1294.
Chen, Y., & Ye, Y. (2014). Effects of salinity and nutrient addition on mangrove Excoecaria agallocha. *PloS one, 9*(4), e93337.
Christensen, S., & Goudriaan, J. (1993). Deriving light interception and biomass from spectral reflectance ratio. *Remote sensing of Environment, 43*(1), 87-95.
Congalton, R. G. (1991). A review of assessing the accuracy of classifications of remotely sensed data. *Remote sensing of Environment, 37*(1), 35-46.
Congalton, R. G., & Green, K. (2008). *Assessing the accuracy of remotely sensed data: principles and practices*: CRC press.
Coppin, P. R., & Bauer, M. E. (1996). Digital change detection in forest ecosystems with remote sensing imagery. *Remote sensing reviews, 13*(3-4), 207-234.
Cornelius, S., Sear, D., Carver, S., & Heywood, D. (1994). GPS, GIS and geomorphological field work. *Earth Surface Processes and Landforms, 19*(9), 777-787.
Cúc, N. T. K. (2013). NGHIÊN CỨU KHẢ NĂNG HẤP THỤ NĂNG LƯỢNG SÓNG CỦA RỪNG NGẬP MẶN TRỒNG TẠI NAM ĐỊNH VÀ THÁI BÌNH.
Dahdouh-Guebas, F. (2001). Mangrove vegetation structure dynamics and regeneration.
Darmawan, S., Takeuchi, W., Vetrita, Y., Winarso, G., Wikantika, K., & Sari, D. (2014). *Characterization of mangrove forest types based on ALOS-PALSAR in overall Indonesian archipelago.* Paper presented at the IOP Conference Series: Earth and Environmental Science.
Dat, P. T., & Yoshino, K. (2011). *Monitoring mangrove forest using multi-temporal satellite data in the Northern Coast of Vietnam.* Paper presented at the the 32nd Asian Conf. on Remote Sensing.
De Vos, W. (2004). Wave attenuation in mangrove wetlands. Red River Delta, Vietnam.
Đỗ Quý, M., & Bùi Thế, Đ. (2018). Bước đầu phân loại lập địa và đánh giá khả năng sinh trưởng, chất lượng rừng trồng ngập mặn ven biển tỉnh Thái Bình.
Draper, N., & Smith, H. (1998). Applied regression analysis: Wiley interscience. *New York*, 505-553.
Eslami-Andargoli, L., Dale, P., Sipe, N., & Chaseling, J. (2009). Mangrove expansion and rainfall patterns in Moreton Bay, southeast Queensland, Australia. *Estuarine, coastal and shelf science, 85*(2), 292-298.
FAO, U. (2007). The world's mangroves 1980–2005. *FAO Forestry Paper*.
Fatoyinbo, T. E., Simard, M., Washington-Allen, R. A., & Shugart, H. H. (2008). Landscape-scale extent, height, biomass, and carbon estimation of Mozambique's mangrove forests with Landsat ETM+ and Shuttle Radar Topography Mission elevation data. *Journal of Geophysical Research: Biogeosciences, 113*(G2).
Foody, G. M., Cutler, M. E., Mcmorrow, J., Pelz, D., Tangki, H., Boyd, D. S., & Douglas, I. (2001). Mapping the biomass of Bornean tropical rain forest from remotely sensed data. *Global Ecology and Biogeography, 10*(4), 379-387.
Gao, J. (1998). A hybrid method toward accurate mapping of mangroves in a marginal

habitat from SPOT multispectral data. *International Journal of Remote Sensing, 19*(10), 1887-1899.
Gilman, E. L., Ellison, J., Duke, N. C., & Field, C. (2008). Threats to mangroves from climate change and adaptation options: a review. *Aquatic botany, 89*(2), 237-250.
Giri, C., Ochieng, E., Tieszen, L. L., Zhu, Z., Singh, A., Loveland, T., . . . Duke, N. (2011). Status and distribution of mangrove forests of the world using earth observation satellite data. *Global Ecology and Biogeography, 20*(1), 154-159.
Giri, C., Pengra, B., Zhu, Z., Singh, A., & Tieszen, L. L. (2007). Monitoring mangrove forest dynamics of the Sundarbans in Bangladesh and India using multi-temporal satellite data from 1973 to 2000. *Estuarine, coastal and shelf science, 73*(1-2), 91-100.
Gitelson, A. A., Kaufman, Y. J., & Merzlyak, M. N. (1996). Use of a green channel in remote sensing of global vegetation from EOS-MODIS. *Remote sensing of Environment, 58*(3), 289-298.
Goh, J., Miettinen, J., Chia, A. S., Chew, P. T., & Liew, S. C. (2014). Biomass estimation in humid tropical forest using a combination of ALOS PALSAR and SPOT 5 satellite imagery. *Asian Journal of Geoinformatics, 13*(4).
Green, E. P., Clark, C. D., Mumby, P. J., Edwards, A. J., & Ellis, A. (1998). Remote sensing techniques for mangrove mapping. *International Journal of Remote Sensing, 19*(5), 935-956.
Hamdan, O., Aziz, H. K., & Hasmadi, I. M. (2014). L-band ALOS PALSAR for biomass estimation of Matang Mangroves, Malaysia. *Remote sensing of Environment, 155*, 69-78.
Hanh, N. T. H. (2016). Studying and Evaluating the Ability to form Carbon Sinks in Biomass of the Pure Sonneratia caseolaris Plantation in the Coastal Area of Tien Lang district, Hai Phong city. *Development*, 1.
Heckenlaible, D., Meyerink, A., Torbert, C., & Lacasse, J. (2007). Landsat 7 (L7) enhanced thematic mapper plus (ETM+ level zero-r distribution product (LORP) data format control book (DFCB): Technical report, Department of the Interior US Geological Survey, Sioux Falls, South Dakota.
Herison, A., Yulianda, F., Kusmana, C., Nurjaya, I. W., & Adrianto, L. (2014). The Existing Condition of Mangrove Region of Avicenia marina, Its: Distribution and Functional Transformation. *Jurnal Manajemen Hutan Tropika, 20*(1), 26-36.
Heumann, B. W. (2011). Satellite remote sensing of mangrove forests: Recent advances and future opportunities. *Progress in Physical Geography, 35*(1), 87-108.
Hoa, N. H. USING LANDSAT IMAGERY AND VEGETATION INDICES DIFFERENCING TO DETECT MANGROVE CHANGE: A CASE IN THAI THUY DISTRICT, THAI BINH PROVINCE.
Hong, P. N., & San, H. T. (1993). *Mangroves of Vietnam* (Vol. 7): Iucn.
Huang, C., Thomas, N., Goward, S. N., Masek, J. G., Zhu, Z., Townshend, J. R., & Vogelmann, J. E. (2010). Automated masking of cloud and cloud shadow for forest change analysis using Landsat images. *International Journal of Remote Sensing, 31*(20), 5449-5464.

Huete, A. R. (1988). A soil-adjusted vegetation index (SAVI). *Remote sensing of Environment, 25*(3), 295-309.

Kamal, M., & Phinn, S. (2011). Hyperspectral data for mangrove species mapping: A comparison of pixel-based and object-based approach. *Remote Sensing, 3*(10), 2222-2242.

Khan, M. N. I., Suwa, R., & Hagihara, A. (2005). Allometric relationships for estimating the aboveground phytomass and leaf area of mangrove Kandelia candel (L.) Druce trees in the Manko Wetland, Okinawa Island, Japan. *Trees, 19*(3), 266-272.

Komiyama, A., Poungparn, S., & Kato, S. (2005). Common allometric equations for estimating the tree weight of mangroves. *Journal of Tropical Ecology, 21*(4), 471-477.

Kumar, L., & Mutanga, O. (2017). Remote sensing of above-ground biomass: Multidisciplinary Digital Publishing Institute.

Kumar, L., Sinha, P., Taylor, S., & Alqurashi, A. F. (2015). Review of the use of remote sensing for biomass estimation to support renewable energy generation. *Journal of Applied Remote Sensing, 9*(1), 097696.

Li, X., Gar-On Yeh, A., Wang, S., Liu, K., Liu, X., Qian, J., & Chen, X. (2007). Regression and analytical models for estimating mangrove wetland biomass in South China using Radarsat images. *International Journal of Remote Sensing, 28*(24), 5567-5582.

Lillesand, T., Kiefer, R. W., & Chipman, J. (2014). *Remote sensing and image interpretation*: John Wiley & Sons.

Litton, C. M., Raich, J. W., & Ryan, M. G. (2007). Carbon allocation in forest ecosystems. *Global Change Biology, 13*(10), 2089-2109.

Lu, D. (2006). The potential and challenge of remote sensing-based biomass estimation. *International Journal of Remote Sensing, 27*(7), 1297-1328.

Lu, D., Chen, Q., Wang, G., Liu, L., Li, G., & Moran, E. (2016). A survey of remote sensing-based aboveground biomass estimation methods in forest ecosystems. *International Journal of Digital Earth, 9*(1), 63-105.

Lugo, A. E., & Patterson-Zucca, C. (1977). The impact of low temperature stress on mangrove structure and growth. *Tropical Ecology, 18*(2), 149-161.

Macleod, R. D., & Congalton, R. G. (1998). A quantitative comparison of change-detection algorithms for monitoring eelgrass from remotely sensed data. *Photogrammetric engineering and remote sensing, 64*(3), 207-216.

Manandhar, R., Odeh, I. O., & Ancev, T. (2009). Improving the accuracy of land use and land cover classification of Landsat data using post-classification enhancement. *Remote Sensing, 1*(3), 330-344.

MAP. (2013). Mangrove Action Project. from https://mangroveactionproject.org

Martinuzzi, S., Gould, W. A., & González, O. M. R. (2007). Creating cloud-free Landsat ETM+ data sets in tropical landscapes: cloud and cloud-shadow removal. *US Department of Agriculture, Forest Service, International Institute of Tropical Forestry. Gen. Tech. Rep. IITF-32., 32*.

Mazda, Y., Magi, M., Kogo, M., & Hong, P. N. (1997). Mangroves as a coastal protection from waves in the Tong King delta, Vietnam. *Mangroves and Salt marshes, 1*(2), 127-135.

McKee, K. L. (1993). Soil physicochemical patterns and mangrove species distribution--reciprocal effects? *Journal of ecology*, 477-487.

Mission, S. R. T. Arc-Second Global https://lta. cr. usgs. gov. *SRTM1Arc (Land Processes Distributed Active Archive Center (LP DAAC), USGS/EROS, accessed November 2016)*.

Mitra, A. (2013). *Sensitivity of mangrove ecosystem to changing climate* (Vol. 62): Springer.

Muchoney, D. M., & Haack, B. N. (1994). Change detection for monitoring forest defoliation. *Photogrammetric engineering and remote sensing, 60*(10), 1243-1252.

Muhd-Ekhzarizal, M., Mohd-Hasmadi, I., Hamdan, O., Mohamad-Roslan, M., & Noor-Shaila, S. (2018). ESTIMATION OF ABOVEGROUND BIOMASS IN MANGROVE FORESTS USING VEGETATION INDICES FROM SPOT-5 IMAGE. *Journal of Tropical Forest Science, 30*(2), 224-233.

Mutanga, O., Adam, E., & Cho, M. A. (2012). High density biomass estimation for wetland vegetation using WorldView-2 imagery and random forest regression algorithm. *International Journal of Applied Earth Observation and Geoinformation, 18*, 399-406.

Newton, A. C., Hill, R. A., Echeverría, C., Golicher, D., Rey Benayas, J. M., Cayuela, L., & Hinsley, S. A. (2009). Remote sensing and the future of landscape ecology. *Progress in Physical Geography, 33*(4), 528-546.

Parkinson, C. L. (2003). Aqua: An Earth-observing satellite mission to examine water and other climate variables. *IEEE Transactions on Geoscience and Remote sensing, 41*(2), 173-183.

Pham, T. D., & Yoshino, K. (2012). *Mangrove analysis using ALOS imagery in Hai Phong City, Vietnam.* Paper presented at the Remote Sensing of the Marine Environment II.

Pham, T. D., & Yoshino, K. (2016). Impacts of mangrove management systems on mangrove changes in the Northern Coast of Vietnam. *Tropics, 24*(4), 141-151.

Pinty, B., & Verstraete, M. (1992). GEMI: a non-linear index to monitor global vegetation from satellites. *Vegetatio, 101*(1), 15-20.

Plourde, L., & Congalton, R. G. (2003). Sampling method and sample placement. *Photogrammetric Engineering & Remote Sensing, 69*(3), 289-297.

Proisy, C., Couteron, P., & Fromard, F. (2007). Predicting and mapping mangrove biomass from canopy grain analysis using Fourier-based textural ordination of IKONOS images. *Remote sensing of Environment, 109*(3), 379-392.

Puri, G. S., Gupta, R., Meher-Homji, V., & Puri, S. (1989). *Forest ecology. Volume 2. Plant form, diversity, communities and succession*: Oxford & IBH Publishing Co. Pvt. Ltd.

Quinn, G. P., & Keough, M. J. (2002). *Experimental design and data analysis for biologists*: Cambridge University Press.

Ramachandra, T., & Ganapathy, S. (2007). Vegetation analysis in Uttara Kannada district using GIS and Remote sensing techniques. *Environmental Information System*.

Regression, G. W. Help| ArcGIS for Desktop [Internet]. Desktop. arcgis. com. 2016 [cited 9 March 2016].

Rönnbäck, P. (1999). The ecological basis for economic value of seafood production supported by mangrove ecosystems. *Ecological Economics, 29*(2), 235-252.

Rwanga, S. S., & Ndambuki, J. (2017). Accuracy assessment of land use/land cover classification using remote sensing and GIS. *International Journal of Geosciences, 8*(04), 611.

Salmo, S. G., Lovelock, C., & Duke, N. C. (2013). Vegetation and soil characteristics as indicators of restoration trajectories in restored mangroves. *Hydrobiologia, 720*(1), 1-18.

Sellers, P., Meeson, B., Hall, F., Asrar, G., Murphy, R., Schiffer, R., . . . Field, C. (1995). Remote sensing of the land surface for studies of global change: Models—algorithms—experiments. *Remote sensing of Environment, 51*(1), 3-26.

Sentinel, E. 1 SAR User Guide (https://sentinel.esa.int/web/sentinel/missions/sentinel-2), 2018. *Cited on*, 53.

sentinel.esa.int. (2018). Spatial and Spectral Resolutions.

Simard, M., Zhang, K., Rivera-Monroy, V. H., Ross, M. S., Ruiz, P. L., Castañeda-Moya, E., . . . Rodriguez, E. (2006). Mapping height and biomass of mangrove forests in Everglades National Park with SRTM elevation data. *Photogrammetric Engineering & Remote Sensing, 72*(3), 299-311.

Sisodia, P. S., Tiwari, V., & Kumar, A. (2014). *Analysis of supervised maximum likelihood classification for remote sensing image.* Paper presented at the Recent Advances and Innovations in Engineering (ICRAIE), 2014.

Song, C., Woodcock, C. E., Seto, K. C., Lenney, M. P., & Macomber, S. A. (2001). Classification and change detection using Landsat TM data: when and how to correct atmospheric effects? *Remote sensing of Environment, 75*(2), 230-244.

Spalding, M., Kainuma, M., & Collins, L. (2010). World atlas of mangroves. A collaborative project of ITTO, ISME, FAO, UNEP-WCMC. *London, UK: Earthscan*.

Spalding, M. D., Blasco, F., & Field, C. D. (1997). World mangrove atlas.

Syed, M. A., Hussin, Y. A., & Weir, M. (2001). *Detecting fragmented mangroves in the Sundarbans, Bangladesh using optical and radar satellite images.* Paper presented at the Paper presented at the 22nd Asian Conference on Remote Sensing.

Tam, N., & Wong, Y. (1996). Retention and distribution of heavy metals in mangrove soils receiving wastewater. *Environmental Pollution, 94*(3), 283-291.

Tang, H., & Mayersohn, M. (2007). Utility of the coefficient of determination (r2) in assessing the accuracy of interspecies allometric predictions: illumination or illusion? *Drug Metabolism and Disposition*.

Thụy, T. V., Thành, P. T., Giang, Đ. H., Dương, P. M., Hà, N. T., & Quốc, N. M. (2016). Nghiên cứu ảnh hưởng của biến đổi khí hậu đến một số hệ sinh thái ven biển tỉnh Thái Bình và khả năng ứng phó. *VNU Journal of Science: Earth and Environmental Sciences, 32*(1S).

Tobias, A., Malabrigo, P., Umali, A. G., Galang, M., Urriza, R., L. Replan, E., & Dida, J. J. (2017). *Mangrove Forest Inventory and Estimation of Carbon Storage and Sedimentation in Pagbilao*.

Tripathi, S., Soni, S. K., Maurya, A. K., & Soni, P. K. (2010). Calculating carbon

sequestration using remote sensing and GIS. *Geospatial world*, 1-8.
usgs.gov. (c2018). Landsat Missions. 18 October, 2018, from https://landsat.usgs.gov/landsat-7
Van Suu, N. (2009). Industrialization and Urbanization in Vietnam: How Appropriation of Agricultural Land Use Rights Transformed Farmers' Livelihoods in a Peri-Urban Hanoi Village? *Final Report of an EADN Individual Research Grant Project, EADN Working Paper, 38*.
VNRC. (2006). Mangrove Reforestation Project to Protect Sea Dyke and Families Living in the Coastal Regions Prone to Natural Disasters of Northern Vietnam., from http://www.livelihoodscentre.org
Vo, Q. T., Oppelt, N., Leinenkugel, P., & Kuenzer, C. (2013). Remote sensing in mapping mangrove ecosystems—An object-based approach. *Remote Sensing, 5*(1), 183-201.
Vo, T. Q., Kuenzer, C., & Oppelt, N. (2015). How remote sensing supports mangrove ecosystem service valuation: A case study in Ca Mau province, Vietnam. *Ecosystem Services, 14*, 67-75.
Wallacea, J. P. K. (2016). REGENERASI ALAMI SEMAI MANGROVE DI AREAL TERDEGRADASI TAMAN NASIONAL KUTAI.
Wenger, K. F. (1984). *Forestry handbook* (Vol. 84): John Wiley & Sons.
Wicaksono, P., Danoedoro, P., Hartono, & Nehren, U. (2016). Mangrove biomass carbon stock mapping of the Karimunjawa Islands using multispectral remote sensing. *International Journal of Remote Sensing, 37*(1), 26-52.
Wilkinson, G. G. (2005). Results and implications of a study of fifteen years of satellite image classification experiments. *IEEE Transactions on Geoscience and Remote sensing, 43*(3), 433-440.
Winarso, G., Vetrita, Y., Purwanto, A. D., Anggraini, N., Darmawan, S., & Yuwono, D. M. (2017). MANGROVE ABOVE GROUND BIOMASS ESTIMATION USING COMBINATION OF LANDSAT 8 AND ALOS PALSAR DATA. *International Journal of Remote Sensing and Earth Sciences (IJReSES), 12*(2), 85-96.
Witenstein, M. M. (1955). *Uses and Limitations of Aerial Photography in Urban Analysis and Planning*: American Society of Photogrammetry.
Yevugah, L. L. (2017). *Spatial mapping of carbon stock in mangroves in the Ellembelle District, Ghana.*
Yinxia, C. (1995). Ecologycal Effects of the Mangrove on the Environment [J]. *Marine Environmental Science, 4*.
Zaitunah, A., Ahmad, A., & Safitri, R. (2018). *Normalized difference vegetation index (ndvi) analysis for land cover types using landsat 8 oli in besitang watershed, Indonesia.* Paper presented at the IOP Conference Series: Earth and Environmental Science.
Zanne, A. E., Lopez-Gonzalez, G., Coomes, D. A., Ilic, J., Jansen, S., Lewis, S. L., . . . Chave, J. (2009). *Data from: Towards a worldwide wood economics spectrum*. Retrieved from: https://doi.org/10.5061/dryad.234
Zheng, D., Rademacher, J., Chen, J., Crow, T., Bresee, M., Le Moine, J., & Ryu, S.-R. (2004). Estimating aboveground biomass using Landsat 7 ETM+ data across a managed landscape in northern Wisconsin, USA. *Remote sensing of*

Environment, *93*(3), 402-411.

APPENDIX

Pictures from Field






AGB in field survey and estimate base on vegetation indices

plot	field AGB	AGB estimated by NDVI	AGB estimated by SAVI	AGB estimated by GNDVI
1	35.44178678	41.324243	41.326733	42.49259
2	56.69417773	54.669153	54.672164	53.212024
3	41.66123379	37.23245	37.234857	37.289552
4	30.17078907	30.474218	30.476327	31.41431
5	14.28737038	32.156409	32.157801	27.829325
6	29.09526802	29.731879	29.730679	14.133884
7	40.9920866	31.891911	31.892985	30.016565
8	40.45927259	45.036226	45.040055	45.579884
9	67.75361843	64.18994	64.194508	63.654709
10	39.51777002	44.804359	44.806654	42.134398
11	15.23279638	24.647205	24.652361	32.422971
12	24.06631545	18.708333	18.713444	29.934138
13	44.98298951	15.952085	15.954022	19.490376
14	55.17515514	57.860944	57.863204	53.48709
15	37.21570124	47.733665	47.735399	46.663268
16	19.64770893	16.416592	16.417087	12.171213
17	12.4459016	24.182898	24.184082	24.284127
18	22.60486588	7.192793	7.192976	3.34719
19	35.17073766	49.351382	49.353629	48.507704
20	46.30490358	55.236737	55.237932	52.375199
21	13.83521569	23.598763	23.600169	24.344472
22	19.70027499	15.249522	15.250207	11.493546
23	21.41467991	19.296593	19.300324	28.8261
24	56.483021	54.702724	54.706293	54.092763
25	39.02586974	47.398908	47.401526	47.72799
26	71.04324146	61.930372	61.935446	64.243286
27	9.939898557	9.022484	9.023973	8.104289
28	40.56633347	51.5225	51.526485	50.954025
29	32.79636695	35.715134	35.717758	37.733145
30	111.3711832	62.188905	62.193951	66.074229
31	18.24733994	8.639684	8.641283	10.697906
32	20.72112338	29.493099	29.494894	29.36577
33	29.4214	33.272765	33.274893	30.00978
34	62.95712136	60.644671	60.649031	61.777098
35	9.570574399	12.26286	12.264417	11.751805
36	9.190311074	11.583554	11.586462	18.561114
37	8.663344669	18.556306	18.557565	17.813792